Nitric oxide–mediated regulation of ferroportin-1 controls macrophage iron homeostasis and immune function in *Salmonella* infection

Manfred Nairz,[1] Ulrike Schleicher,[4] Andrea Schroll,[1] Thomas Sonnweber,[1] Igor Theurl,[1] Susanne Ludwiczek,[1] Heribert Talasz,[2] Gerald Brandacher,[5] Patrizia L. Moser,[3] Martina U. Muckenthaler,[6] Ferric C. Fang,[7] Christian Bogdan,[4] and Günter Weiss[1]

[1]Department of Internal Medicine VI, Infectious Diseases, Immunology, Rheumatology, Pneumology; [2]Biocenter, Division of Clinical Biochemistry; [3]Department of Pathology, Medical University of Innsbruck, 6020 Innsbruck, Austria
[4]Mikrobiologisches Institut – Klinische Mikrobiologie, Immunologie und Hygiene, Universitätsklinikum Erlangen und Friedrich-Alexander-Universität Erlangen-Nürnberg, 91054 Erlangen, Germany
[5]Department of Plastic and Reconstructive Surgery, Johns Hopkins University School of Medicine, Baltimore, MD 21287
[6]Department of Pediatric Oncology, Hematology, and Immunology, University of Heidelberg, D-69120 Heidelberg, Germany
[7]Departments of Laboratory Medicine and Microbiology, University of Washington, Seattle, WA 98195

Nitric oxide (NO) generated by inducible NO synthase 2 (NOS2) affects cellular iron homeostasis, but the underlying molecular mechanisms and implications for NOS2-dependent pathogen control are incompletely understood. In this study, we found that NO up-regulated the expression of ferroportin-1 (Fpn1), the major cellular iron exporter, in mouse and human cells. *Nos2*$^{-/-}$ macrophages displayed increased iron content due to reduced Fpn1 expression and allowed for an enhanced iron acquisition by the intracellular bacterium *Salmonella typhimurium*. *Nos2* gene disruption or inhibition of NOS2 activity led to an accumulation of iron in the spleen and splenic macrophages. Lack of NO formation resulted in impaired nuclear factor erythroid 2–related factor-2 (Nrf2) expression, resulting in reduced Fpn1 transcription and diminished cellular iron egress. After infection of *Nos2*$^{-/-}$ macrophages or mice with *S. typhimurium*, the increased iron accumulation was paralleled by a reduced cytokine (TNF, IL-12, and IFN-γ) expression and impaired pathogen control, all of which were restored upon administration of the iron chelator deferasirox or hyperexpression of Fpn1 or Nrf2. Thus, the accumulation of iron in *Nos2*$^{-/-}$ macrophages counteracts a proinflammatory host immune response, and the protective effect of NO appears to partially result from its ability to prevent iron overload in macrophages

CORRESPONDENCE
Guenter Weiss:
guenter.weiss@i-med.ac.at

Abbreviations used: ACD, anemia of chronic disease; ARE, antioxidant response element; Bmp, bone morphogenic protein; DFO, desferroxamine; DFX, deferasirox; Dmt1, divalent metal transporter 1; EmGFP, Emerald green-fluorescent protein; Fpn1, ferroportin-1; Ft, ferritin; IRE, iron-responsive element; IRP, iron regulatory protein; MOI, multiplicity of infection; NF, nuclear factor; Nramp1, natural resistance-associated macrophage protein 1; Nrf2, NF erythroid 2-related factor 2; PAMP, pathogen-associated molecular pattern; PE-MΦ, peritoneal exudate macrophage; *S. typhimurium*, *Salmonella enterica* serovar Typhimurium; Tfr1, transferrin receptor 1.

Iron homeostasis and nitric oxide (NO) biology are reciprocally interconnected. Iron affects the expression of inducible or type 2 NO synthase 2 (iNOS or NOS2) by negatively modulating the binding affinity of the iron-sensitive transcription regulators hypoxia-inducible factor (HIF) and nuclear factor (NF)-IL6 to their respective consensus sequences within the *Nos2* promoter (Weiss et al., 1994; Melillo et al., 1997; Dlaska and Weiss 1999). This is important to the host immune response because NOS2 is a major component of the antimicrobial effector machinery, and the formation of NO by macrophages has been shown to mediate protection from infections with a myriad of pathogens, including viruses, bacteria, protozoa, and parasites (MacMicking et al., 1997; Bogdan, 2001). Some of these effects have been linked to direct cellular toxicity exerted by the labile radical NO and its chemical congeners, which are generated upon interaction with reactive oxygen intermediates (Stamler and Hausladen, 1998). In addition, the high affinity of NO for iron leads to targeting of heme and nonheme iron and destabilization of iron-sulfur clusters within the

The Rockefeller University Press $30.00
J. Exp. Med. 2013 Vol. 210 No. 5 855-873
www.jem.org/cgi/doi/10.1084/jem.20121946

The Journal of Experimental Medicine

active centers of enzymes that are crucial for DNA synthesis and metabolic processes (Drapier and Hibbs, 1988). Moreover, NO controls cellular iron homeostasis by activating iron regulatory protein-1 (IRP1). IRP1 binds to specific RNA stem–loop structures termed iron-responsive elements (IREs), which are located within the 3′- or 5′-untranslated regions of genes that play critical roles in iron metabolism, thereby controlling their posttranscriptional expression. Activation of IRP1 binding to IREs by NO prolongs the mRNA half-life of transferrin receptor 1 (Tfr1), leading to increased iron uptake, and at the same time inhibits the mRNA translation of the iron-storage protein ferritin (Ft), so that the concentration of free intracellular iron increases (Drapier et al., 1993; Weiss et al., 1993; Wardrop et al., 2000; Wang et al., 2005).

Cellular iron homeostasis in macrophages is regulated at multiple steps and by numerous genes (Weiss, 2009). Macrophages can acquire iron by Tfr1-mediated uptake of transferrin-bound iron, acquisition of molecular iron via the divalent metal transporter 1 (Dmt1) and, most importantly, phagocytosis of senescent erythrocytes with subsequent recycling of iron. The diversion of cellular iron is then orchestrated by the IRP/IRE interaction resulting in iron reutilization, iron storage within Ft or iron export. Importantly, there is only one well-characterized pathway by which iron can exit cells, ferroportin-1 (Fpn1), which is expressed on the cell surface of macrophages, hepatocytes, duodenal enterocytes, and erythroid progenitors and acts as the exclusive trans-membrane export protein for ferrous (Fe^{2+}) iron (Abboud and Haile, 2000; Donovan et al., 2000; McKie et al., 2000). Thus, Fpn1 expression is a key determinant of cellular iron content. Hepcidin, a mainly liver-derived peptide induced by iron and cytokines and master regulator of body iron homeostasis, exerts its regulatory effects via binding to Fpn1, which is thought to be the hepcidin receptor. This interaction results in Fpn1 internalization, proteasomal degradation and blockage of iron export (Nemeth et al., 2004).

There are two splicing variants of Fpn1 in mammalian cells. Many cell types, including macrophages, mainly express the Fpn1 mRNA variant (Fpn1A), which harbors an IRE within its 5′-untranslated region (Hentze et al., 2004), thus making it susceptible to IRP-mediated translational regulation. In contrast, duodenal enterocytes and erythroid progenitor cells exclusively express the Fpn1B transcript, which lacks this IRE (Zhang et al., 2009).

The expression of these crucial mediators of iron homeostasis is significantly affected during infection and inflammation. Cytokines such as IL-6 or IL-1β, in concert with LPS, induce the expression of hepcidin to result in cellular Fpn1 degradation. This causes iron restriction within macrophages, blockage of duodenal iron export into the circulation, and the development of hypoferremia (Hentze et al., 2004; Kemna et al., 2005; Nemeth and Ganz, 2006).

In addition, cytokines stimulate the expression of iron uptake genes Tfr1 and Dmt1, while inhibiting Fpn1 transcription, with the net result of macrophage iron retention (Yang et al., 2002; Ludwiczek et al., 2003). Also, macrophages can produce small amounts of hepcidin in response to IL-6 or pathogen-associated molecular patterns (PAMPs), resulting in autocrine inhibition of macrophage iron efflux (Armitage et al., 2011). These inflammation-mediated effects on iron homeostasis reflect a defense strategy of the body to limit iron availability for invading extracellular pathogens, which require the metal for their growth and pathogenicity (Ganz, 2009; Nairz et al., 2010).

The iron retention in macrophages, however, bears the risk of improved iron supply to intracellular pathogens (Ganz, 2009; Nairz et al., 2010). In addition, the infected host organism can develop an anemia of chronic disease (ACD) as the restriction of iron also impairs the erythropoiesis (Weiss and Goodnough, 2005). Moreover, cellular iron retention is associated with reduced production of TNF and IL-6 by inflammatory monocytes and macrophages (Oexle et al., 2003; Nairz et al., 2009a). Thus, via increasing macrophage iron content, hepcidin might have immunomodulatory effects (Pagani et al., 2011).

Given the established regulatory circuits between NOS2 activity and iron homeostasis, and considering the important roles of both molecules for the course of infection, we hypothesized that part of the protective effect of NOS2-derived NO during infections might result from the modulation of macrophage iron content and systemic iron homeostasis.

RESULTS

Nos2-deficient macrophages have increased iron content and reduced Fpn1 expression

We first isolated thioglycolate-elicited primary peritoneal exudate macrophages (PE-MΦ) from $Nos2^{+/+}$ and $Nos2^{-/-}$ mice. $Nos2^{-/-}$ PE-MΦ had significantly higher cellular iron content as compared with $Nos2^{+/+}$ cells (Fig. 1 A). Although hepcidin mRNA levels were comparable, $Nos2^{-/-}$ PE-MΦ showed reduced Fpn1 mRNA expression (Fig. 1 B). To investigate the temporal regulation of iron metabolic genes in response to NO, wild-type macrophages were stimulated with NO donors of two different chemical classes, i.e., the oxide Nor5 and the oxatriazole GEA5583 (unpublished data), which provided similar results. The addition of Nor5 to wild-type macrophages resulted in a significant time-dependent increase in Fpn1 mRNA and protein levels (Fig. 1, C–E), whereas hepcidin levels were not significantly affected (Fig. 1 F).

Next, we asked whether NO alters Fpn1 mRNA half-life or affects Fpn1 transcription. Primary macrophages stimulated with Nor5 or solvent for 6 h and subsequently exposed to actinomycin D for different time periods showed comparable decay of Fpn1 mRNA with a calculated Fpn1 mRNA half-life of ∼3 h for both treatments (unpublished data).

Using a dual luciferase reporter system, we found that Nor5-treatment resulted in a significant induction of Fpn1 transcription in cells transiently transfected with the full-length 8.4-kb murine Fpn1 promoter lacking an IRE so that iron/IRP/IRE-mediated effects on mRNA stability could be excluded (Fig. 1 G, right). In contrast, no effect was observed in cells transfected with the empty pGL3 reporter plasmid (Fig. 1 G, left). To see whether

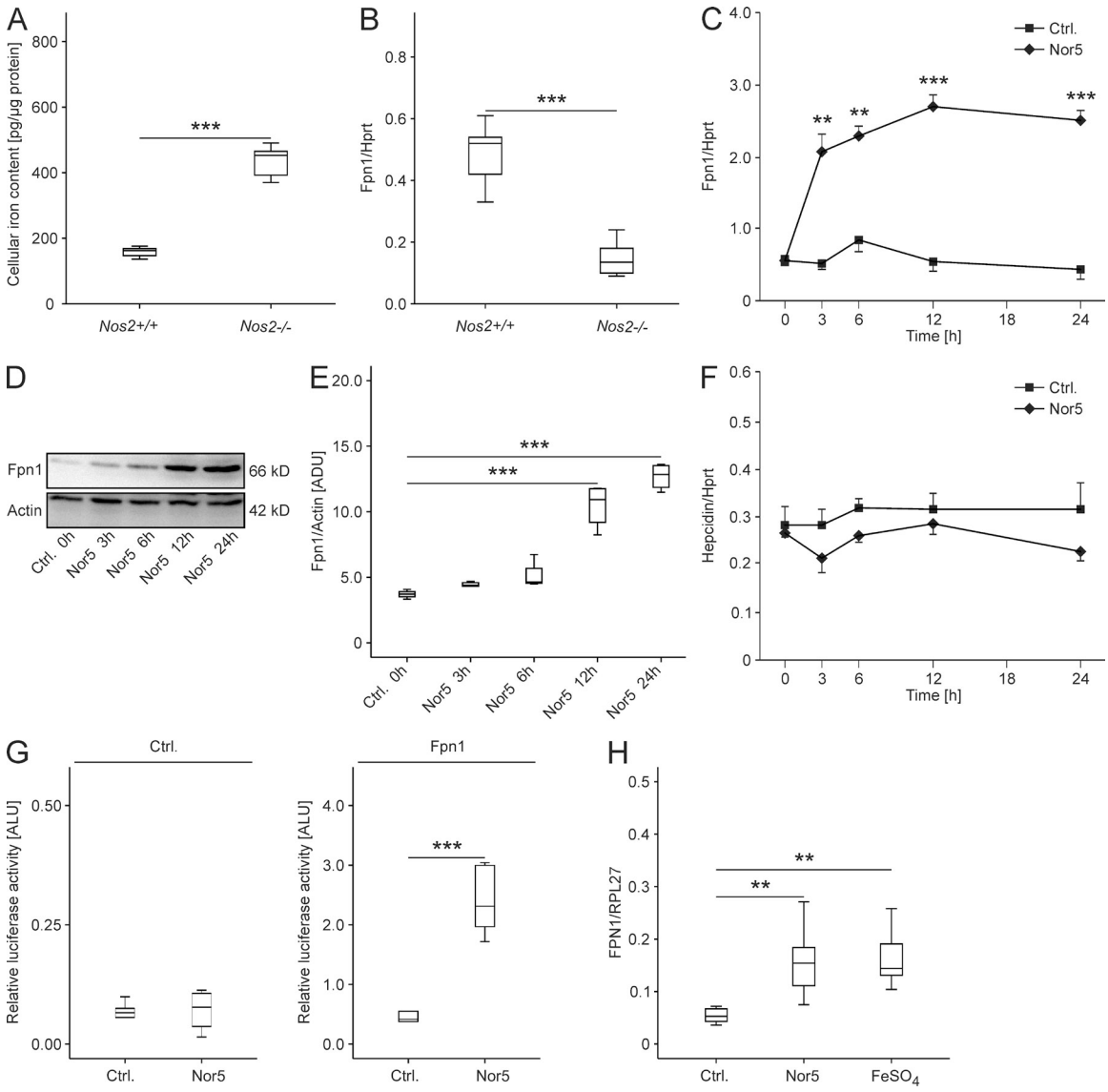

Figure 1. Iron content and ferroportin-1 expression in primary *Nos2*$^{+/+}$ and *Nos2*$^{-/-}$ PE-MΦ. (A) Cellular iron content of primary *Nos2*$^{+/+}$ and *Nos2*$^{-/-}$ PE-MΦ was measured by atomic absorption spectrometry. Results were normalized for protein content and compared by Student's *t* test. Values are depicted as lower quartile, median, and upper quartile (boxes) with minimum and maximum ranges and statistical significance between *Nos2*$^{+/+}$ and *Nos2*$^{-/-}$ cells indicated (PE-MΦ isolated from $n = 9$ individual mice per group). (B) Quantitative RT-PCR (qRT-PCR) was used to analyze Fpn1 mRNA levels. Data, normalized for mRNA levels of the housekeeping gene Hprt, were compared and are depicted as in A (PE-MΦ isolated from $n = 9$ individual mice per group). (C–F) Wild-type PE-MΦ were stimulated with 50 µM of the NO donor Nor5 for different time periods, as indicated. (C) Fpn1 expression was determined by qRT-PCR. Data were compared and are depicted as mean and SEM ($n = 4$ independent experiments). (D) Western blotting was used to assess Fpn1 protein expression. Actin expression was assessed by reprobing membranes and is shown as loading control. One of four independent experiments is depicted. (E) Fpn1 and actin levels were quantified by densitometric scanning of membranes. Data were compared by ANOVA using Bonferroni's correction ($n = 4$ independent experiments). (F) Hepcidin mRNA expression was assessed by means of qRT-PCR and data are presented as described for Fpn1 ($n = 4$ independent experiments). (G) Activation of the 8.4-kb full-length murine Fpn1 promoter Firefly reporter construct in response to Nor5 was measured in a dual luciferase assay (right) using co-transfection with the Renilla luciferase pRL-SV40 vector as reference. Cells transfected with the empty pGL3 reporter plasmid served as controls (left). Firefly luciferase activity was normalized to Renilla luciferase activity and is depicted as relative activity in arbitrary light units (ALU; $n = 4$ independent experiments). (H) Primary human CD14$^+$ monocytes were exposed to solvent, Nor5 (50 µM), or $FeSO_4$ (50 µM) for 6 h and FPN1 mRNA expression was quantified by means of qRT-PCR and normalized for levels of the housekeeping gene RPL27 (cells of $n = 7$ individual subjects). **, $P < 0.01$; ***, $P < 0.001$.

these effects also occur in human cells, CD14$^+$ monocytes were isolated from peripheral blood of healthy volunteers and stimulated with Nor5. Of note, Nor5 resulted in a substantial induction of FPN1 mRNA expression (Fig. 1 H), as did iron sulfate ($FeSO_4$). These data suggest that NOS2-derived NO mediates iron export via transcriptional up-regulation of Fpn1.

NOS2 activity is required for Fpn1-dependent iron restriction in *Salmonella*-infected macrophages

Next, we evaluated the putative contribution of NOS2 to the induction of Fpn1 in response to infection with the intracellular bacterium *Salmonella enterica* serovar Typhimurium (*S. typhimurium*). Wild-type PE-MΦ were infected with *S. typhimurium* at a multiplicity of infection (MOI) of 10 and treated with the NOS2 inhibitor L-NIL. As published earlier (Nairz et al., 2007), the infection resulted in an up-regulation of the Fpn1 mRNA and protein expression. This effect, however, was blocked by the addition of L-NIL to *S. typhimurium*–infected macrophages (Fig. 2, A–C). In parallel, the cellular iron release was significantly reduced in *S. typhimurium*–infected macrophages concurrently treated with L-NIL (Fig. 2 D).

As the induction of Fpn1 is a mechanism for depriving intracellular microbes of iron (Ganz, 2009; Nairz et al., 2010), we evaluated the effect of NOS2 inhibition on the ability of *S. typhimurium* to acquire iron within infected macrophages. We observed that L-NIL resulted in a substantial increase in the access of intracellular *Salmonella* to radioactive ferrous iron added to infected PE-MΦ (Fig. 2 E), whereas it did not affect iron acquisition by *Salmonella* grown in liquid cultures (Fig. 2 F).

Salmonella-induced expression of Fpn1 is dependent on NO and Nrf2

Next, we investigated the mechanisms underlying NO-mediated induction of Fpn1 expression. Fpn1 transcription is stimulated by NF erythroid 2-related factor-2 (Nrf2), which binds to an antioxidant response element (ARE) within the Fpn1 promoter (Marro et al., 2010; Harada et al., 2011). *Salmonella* infection of wild-type PE-MΦ resulted in a significant activation of Nrf2 binding, which was impaired upon addition of L-NIL (Fig. 2 G).

When analyzing cells transiently transfected with Fpn1 promoter reporter constructs, we observed that *Salmonella* infection resulted in a significant induction of Fpn1 in comparison to solvent-treated cells (Fig. 2 H). This induction was dependent on the presence of an intact Nrf2-binding sequence within the Fpn1 promoter and on the production of NO. From these data, we conclude that *Salmonella*-infected macrophage increase iron export due to the up-regulation of Fpn1 expression that results from an NO-dependent binding of Nrf2 to the Fpn1 promoter and limits the bacterial access to iron.

NOS2 mediates antibacterial activity of macrophages via iron restriction

To further explore the idea that an altered iron homeostasis contributes to the well-known susceptibility of $Nos2^{-/-}$ macrophages to infections with intracellular bacteria, PE-MΦ from $Nos2^{+/+}$ and $Nos2^{-/-}$ mice were infected with *S. typhimurium*. In line with the data obtained with uninfected macrophages (Fig. 1), $Nos2^{+/+}$ PE-MΦ expressed higher amounts of Fpn1 protein (Fig. 3, A and B). Furthermore, in transiently transfected PE-MΦ, the 8.4-kb Fpn1 promoter construct was more efficiently transcribed in $Nos2^{+/+}$ than in $Nos2^{-/-}$ macrophages after bacterial infection (Fig. 3 C). Accordingly, iron release from *Salmonella*-infected $Nos2^{-/-}$ cells was significantly lower as compared with their $Nos2^{+/+}$ counterparts (Fig. 3 D).

As previously described (Shiloh et al., 1999), the bacterial load of *Salmonella*-infected $Nos2^{-/-}$ macrophages was higher than that of $Nos2^{+/+}$ macrophages (Fig. 3 E). We therefore tested whether iron depletion could reverse this phenotype. Indeed, treatment of *Salmonella*-infected PE-MΦ with the iron chelator deferasirox (DFX) resulted in a significant reduction of the number of intracellular *Salmonella* and virtually eliminated the differences in *Salmonella* survival between $Nos2^{-/-}$ and $Nos2^{+/+}$ macrophages (Fig. 3 E).

The addition of IFN-γ to *Salmonella*-infected RAW264.7 macrophage-like cells resulted in a further induction of Fpn1 mRNA levels, as did the overexpression of functional natural resistance-associated macrophage protein 1 ($Nramp1^R$; Fig. 3 F). NOS2-derived NO was required for both effects, as L-NIL prevented the up-regulation of Fpn1 and the subsequent reduction of macrophage iron content (Fig. 3, F and G).

The increased capacity of DFX-treated $Nos2^{-/-}$ macrophages to control intracellular *Salmonella* proliferation was associated with an up-regulation of the proinflammatory cytokine TNF. Also, DFX abrogated the differences otherwise observed between $Nos2^{+/+}$ and $Nos2^{-/-}$ macrophages (unpublished data).

As a complementary approach, $Nos2^{+/+}$ and $Nos2^{-/-}$ PE-MΦ were transiently transfected with three different FPN1 expression plasmids. Western blots confirmed the expression of high Fpn1 protein levels in transfected control cells of either *Nos2* genotype (Fig. 4, A and B). The overexpression of wild-type FPN1 or a N144H mutant FPN1, which is insensitive to hepcidin-mediated degradation (Drakesmith et al., 2005), resulted in a significant and comparable reduction of intracellular *Salmonella* survival and abrogated the differences in bacterial counts seen between untransfected $Nos2^{+/+}$ and $Nos2^{-/-}$ macrophages. In contrast, overexpression of a A77D FPN1 mutant that, unlike wild-type FPN1 and the N144H FPN1 mutant, is not expressed on the cell surface but retained in the endoplasmatic reticulum, had no effect on differences in bacterial numbers between $Nos2^{+/+}$ and $Nos2^{-/-}$ macrophages (Fig. 4 C). Moreover, transfection of cells with wild-type FPN1 and the N144H variant resulted in increased TNF and IL-12p70 secretion after infection with *S. typhimurium* (Fig. 4, D and E).

Supernatants from macrophages transiently transfected with empty p-cDNA3.1 plasmid or human FPN1 constructs were analyzed for the accumulation of nitrite after *S. typhimurium* infection. Overexpression of wild-type FPN1 resulted in a significant increase of nitrite accumulation in culture supernatants. The same phenotype was observed in cells expressing the FPN1 N144H mutant and in macrophages transfected with an empty plasmid vector but treated with DFX. Conversely, the stimulatory effects of wild-type FPN1 overexpression were abrogated upon addition of 50 μM $FeSO_4$ or 1 μM

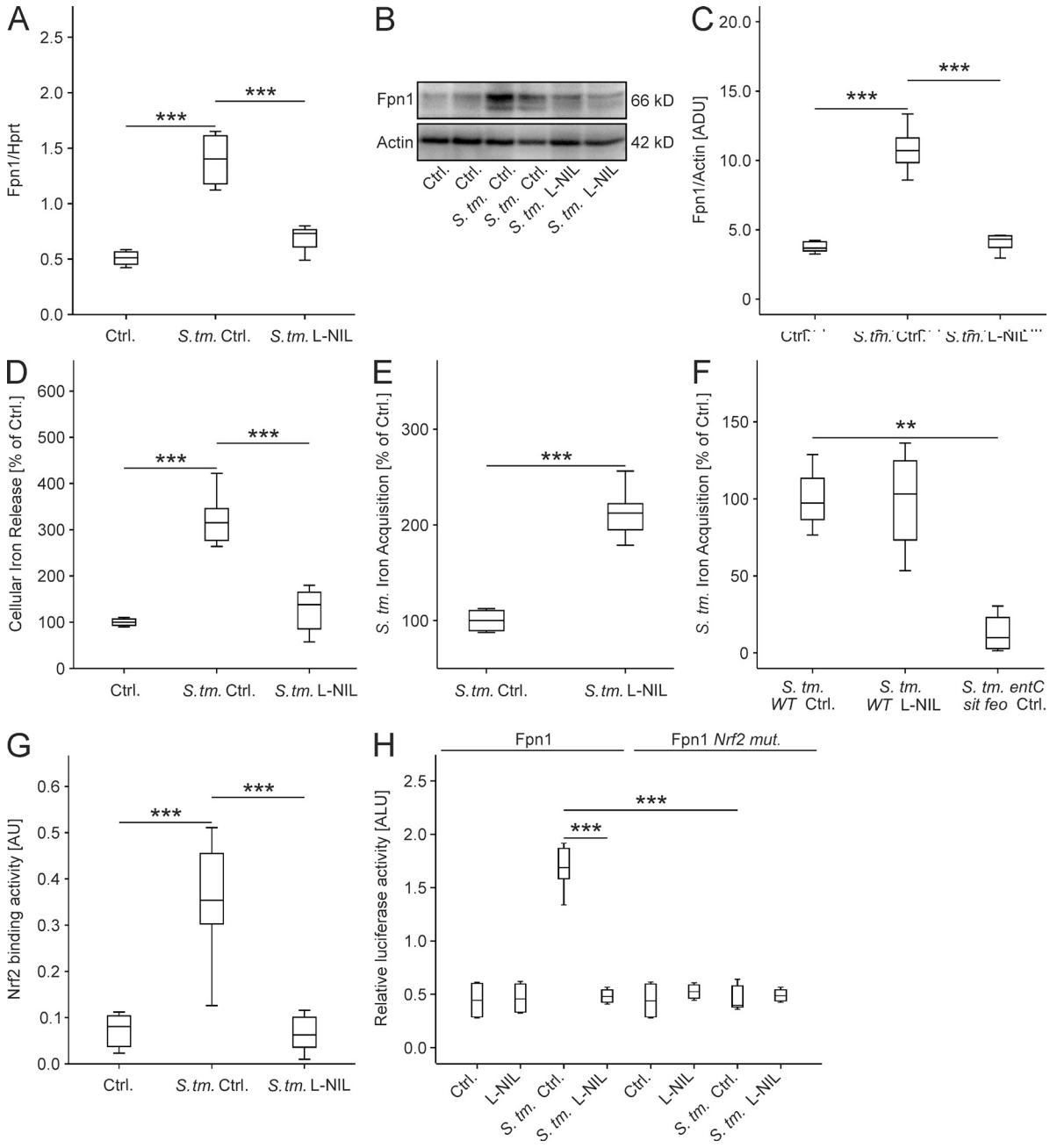

Figure 2. Fpn1 expression, macrophage iron release, and bacterial iron acquisition after pharmacological blockade of NO formation. (A–C) *Nos2*$^{+/+}$ PE-MΦ were infected with *Salmonella typhimurium* (*S. tm.*) and treated with PBS or 600 µM of the NOS2 inhibitor L-NIL for 24 h. (A) Fpn1 expression was determined by qRT-PCR, and data were normalized for mRNA levels of Hprt and compared by ANOVA using Bonferroni's correction for multiple tests. Values are depicted as lower quartile, median, and upper quartile (boxes) with minimum and maximum ranges and statistically significant differences are indicated ($n = 4$ independent experiments). (B) Fpn1 and actin protein levels were assessed by Western blotting, with one of four independent experiments shown. (C) Fpn1 and actin levels were quantified by densitometric scanning of membranes ($n = 8$ independent experiments). (D–F) ^{59}Fe transport studies were used to determine macrophage iron release and bacterial iron acquisition within macrophages and in liquid culture, respectively. (D) After loading with 10 µM ^{59}Fe-citrate, macrophage iron release was determined ($n = 6$ independent experiments). (E) Bacterial iron acquisition within macrophages was determined after loading of infected macrophages with 10 µM ^{59}Fe-citrate. Data were normalized for *Salmonella* numbers as determined by plate counting ($n = 6$ independent experiments). (F) Bacterial iron acquisition in liquid culture was determined after incubation with 10 µM ^{59}Fe-citrate. As control, an isogenic triple mutant, deficient in enterobactin synthesis, sitABCD-, and feo-mediated iron uptake (*S. tm. entC sit feo*) was used. Data are depicted relative to the solvent-treated control (Ctrl.) as described in A ($n = 4$ independent experiments). (G) Wild-type PE-MΦ were infected with *Salmonella typhimurium* (*S. tm.*) and Nrf2-binding activity was determined by a commercially available assay and depicted as arbitrary units (AU; $n = 8$–10 independent experiments). (H) Wild-type PE-MΦ were transiently transfected with an 8.4-kb Fpn1 promoter luciferase construct (Fpn1 8.4-kb), a variant carrying a specific mutation in the Nrf2-binding site (*Nrf2 mut.*), or empty plasmid (not depicted), and subsequently treated with PBS or infected with *S. typhimurium* (*S. tm.*). Luciferase activity is expressed as arbitrary light units (ALU; $n = 4$ independent experiments). **, $P < 0.01$; ***, $P < 0.001$.

synthetic human hepcidin (Fig. 4 F). Together, these data show that the iron overload and the increased survival of *Salmonella* seen in *Nos2*$^{-/-}$ macrophages can be fully reversed by iron chelation or forced iron export. In addition, iron depletion also restored the proinflammatory cytokine response of *Nos2*$^{-/-}$ macrophages.

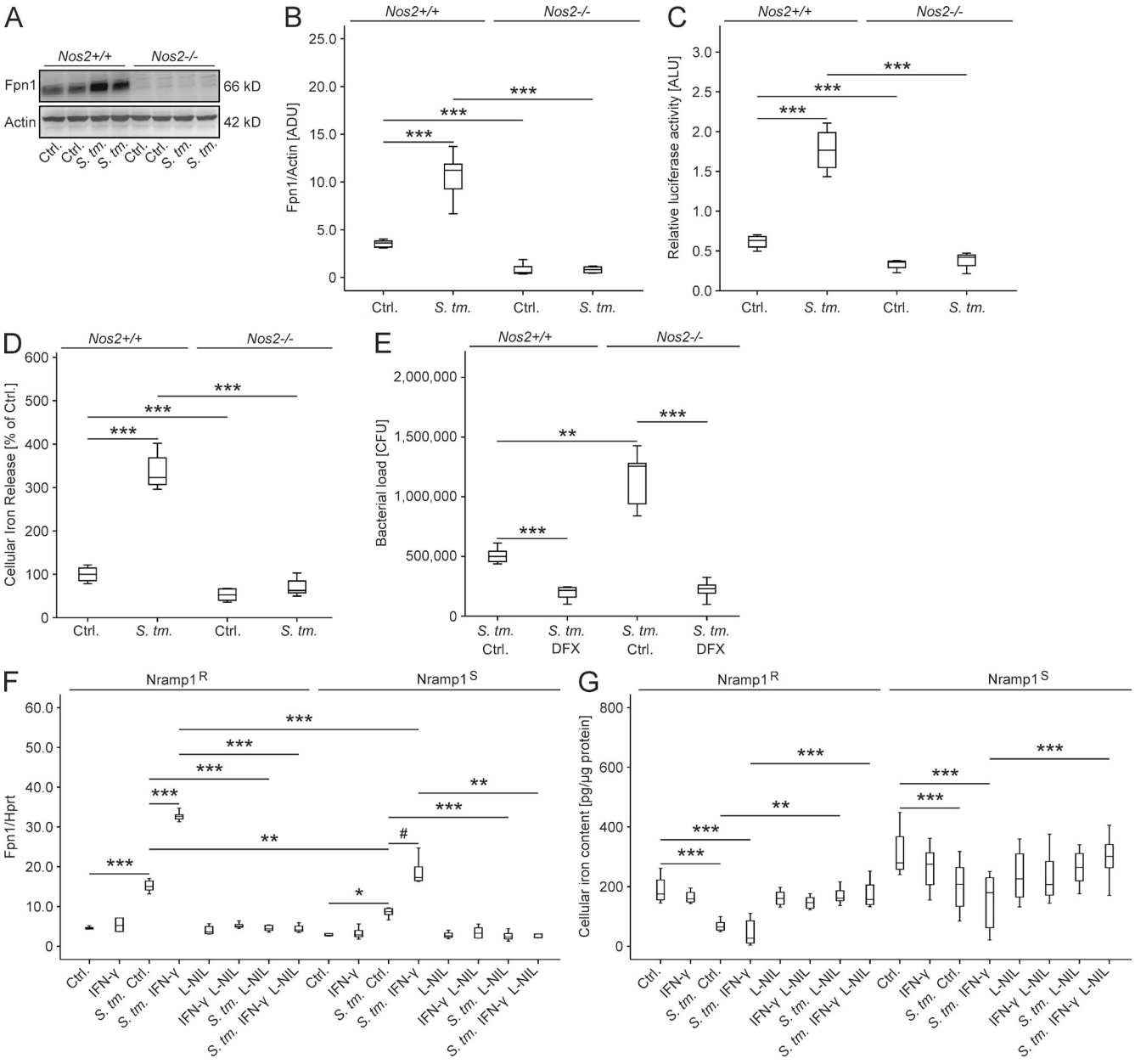

Figure 3. Fpn1 expression and effects of DFX on effector functions in *Nos2*$^{+/+}$ and *Nos2*$^{-/-}$ PE-MΦ. (A and B) *Nos2* wild-type and *Nos2*$^{-/-}$ PE-MΦ were isolated and treated with PBS or infected with *S. typhimurium* (*S. tm.*). (A) Fpn1 in comparison to actin protein expression was determined by means of Western blotting. Data from one of four independent experiments are shown. (B) Fpn1 and actin levels were quantified by densitometric scanning of membranes. Data were compared by ANOVA using Bonferroni's correction (n = 8 independent experiments). (C) PE-MΦ were transiently transfected with the 8.4-kb Fpn1 promoter firefly luciferase construct and pRL-SV40 Renilla luciferase plasmid and infected with *S. typhimurium*. Relative chemiluminescence values are depicted (n = 4 independent experiments). (D) ^{59}Fe release in response to *S. typhimurium* infection was determined after loading of infected macrophages with 10 µM ^{59}Fe-citrate. Data were compared and are depicted as in Fig. 2 D (n = 6 independent experiments). (E) *Nos2*$^{+/+}$ and *Nos2*$^{-/-}$ PE-MΦ were infected and treated with PBS or 50 µM of the iron chelator DFX. Intracellular bacterial load was determined by plating (n = 5–6 independent experiments). (F and G) Fpn1 expression and iron content in RAW264.7 cells expressing (Nramp1^{R}) or lacking functional Nramp1 (Nramp1^{S}) was determined after infection with *S. typhimurium* and stimulation with 10 ng/ml IFN-γ or 600 µM L-NIL. (F) Fpn1 expression was determined by qRT-PCR and data were normalized for mRNA levels of Hprt (n = 6 independent experiments). (G) Cellular iron content of RAW264.7 Nramp1^{R}-expressing cells as compared with RAW264.7 Nramp1^{S}-expressing cells was measured by atomic absorption spectrometry. Results were normalized for protein content (n = 12 independent experiments). #, P < 0.10; *, P < 0.05; **, P < 0.01; ***, P < 0.001.

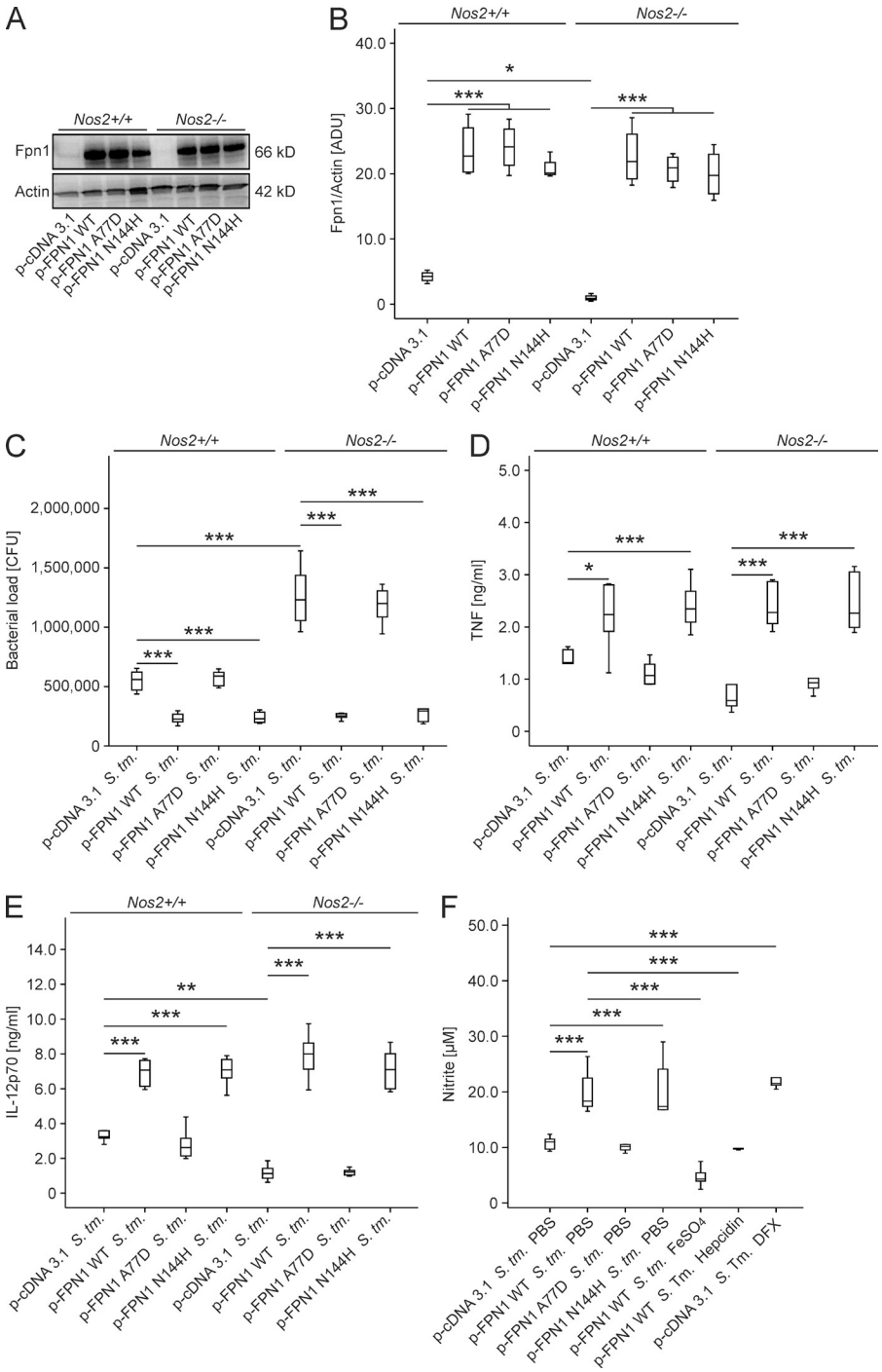

Figure 4. Overexpression of Fpn1 variants and immune functions in *Nos2*$^{+/+}$ and *Nos2*$^{-/-}$ PE-MΦ. (A and B) *Nos2* wild-type and *Nos2*$^{-/-}$ PE-MΦ were transiently transfected with empty plasmid (p-cDNA3.1) or expression constructs containing the indicated human FPN1 variants. (A) Fpn1 protein levels were determined by Western blotting, with one of four independent experiments shown. Actin expression was assessed by reprobing membranes and is shown as loading control. (B) Fpn1 and actin levels were quantified by densitometric scanning of membranes. Data were compared by ANOVA using Bonferroni's correction ($n = 4$ independent experiments). (C–E) The bacterial load in macrophages was quantified by plating of cells lysed with 0.1% SDS on LB agar (C) and the accumulation of TNF (D) and IL-12p70 (E) in cell culture supernatants was measured by ELISA kits ($n = 6$ independent experiments). (F) Nitrite levels were measured in culture supernatants of *Nos2* wild-type PE-MΦ transiently transfected with the indicated plasmids, infected with *S. typhimurium* (*S. tm.*) and treated with PBS, 50 µM $FeSO_4$, 1 µM recombinant murine hepcidin or 50 µM DFX ($n = 4$–6 independent experiments). *, $P < 0.05$; ***, $P < 0.001$.

Having seen that in uninfected macrophages NOS2-derived NO regulates the expression of Fpn1 via the nuclear protein Nrf2 (Fig. 2), we tested whether the same regulatory circuit also holds true in *Salmonella*-infected macrophages. As expected from the NOS2 inhibitor data (Fig. 2), Nrf2 activity was significantly higher in *Nos2*$^{+/+}$ as compared with *Nos2*$^{-/-}$ cells (Fig. 5 A). Furthermore, overexpression of Nrf2, which is paralleled by enhanced transcriptional binding activity (unpublished data), caused a significant increase in iron release from *Salmonella*-infected macrophages (Fig. 5 B). In parallel, the intracellular bacterial loads were significantly reduced after Nrf2 hyperexpression in *Nos2*$^{+/+}$ or *Nos2*$^{-/-}$ macrophages (Fig. 5 C). The reduction of *Salmonella* growth within macrophages overexpressing Nrf2 most likely results from an Fpn1-mediated limitation of bacterial iron access, because it was abrogated upon addition of synthetic murine hepcidin which mediates the degradation of Fpn1 (Fig. 5 D).

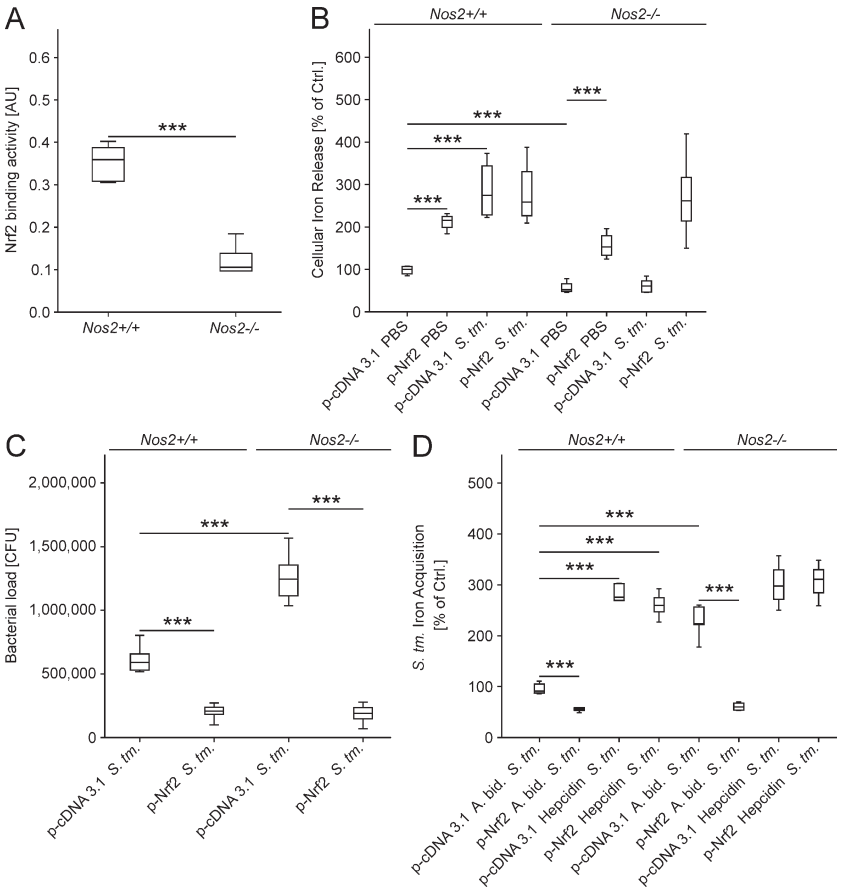

Figure 5. Endogenous Nrf2-binding activity and overexpression of Nrf2 in *Nos2* wild-type and *Nos2*$^{-/-}$ PE-MΦ. (A) The binding affinity of Nrf2 in *Nos2* wild-type and *Nos2*$^{-/-}$ PE-MΦ was determined by a commercially available assay. Data are expressed as arbitrary units [AU], with results depicted as in Fig. 1 A (n = 10 individual mice per group). (B and C) PE-MΦ of the indicated genotypes were transiently transfected with a murine Nrf2 expression plasmid or empty vector (p-cDNA3.1) and subsequently treated with PBS or infected with *S. typhimurium*. Release of ^{59}Fe was measured in a γ-counter (B; n = 4–6 independent experiments). In parallel experiments, the bacterial load in macrophages was determined by plating serially diluted macrophage lysates (C; n = 6–8 independent experiments). (D) ^{59}Fe acquisition by engulfed bacteria was measured in a γ-counter after transient transfection and addition of 1 µM of synthetic hepcidin or distilled water (A. bid.; n = 4–5 independent experiments). ***, $P < 0.001$.

Improved control of *Salmonella* by individual macrophages hyperexpressing Fpn1

To analyze the impact of Fpn1 expression on the antimicrobial activity of macrophages on a single-cell level, we transiently transfected PE-MΦ with plasmids coding for FPN1 and Emerald green fluorescent protein (EmGFP) linked to the N or C terminus of FPN1 or to respective control plasmids lacking FPN1. After infection with *S. typhimurium*, macrophages were evaluated for their expression of GFP and categorized into four groups based on their infection status (i.e., 0, 1–2, 3–5, and >5 bacteria/macrophage) using multicolor immunofluorescence analysis.

In GFP$^+$ macrophages, the expression of FPN1 resulted in lower bacterial loads on a single-cell basis compared with FPN1-negative controls (Fig. 6, A and B, compare right and left panels). Furthermore, many GFP$^-$ cells treated with L-NIL contained at least three bacteria per cell, whereas most GFP$^+$ cells (i.e., FPN1$^+$ cells) did not contain more than two bacteria (Fig. 6, C and D, compare right and left panels). Similarly, most GFP$^+$ *Nos2*$^{+/+}$ macrophages overexpressing FPN1 contained two or fewer bacteria (Fig. 7, A [right] and D), whereas in GFP$^-$ *Nos2*$^{+/+}$ macrophages, the proportion of cells containing 3–5 bacteria was significantly higher (Fig. 7, A [right] and C). As expected, in *Nos2*$^{-/-}$ macrophages the differences between GFP$^+$ cells overexpressing FPN1 (Fig. 7, B [right] and F) and GFP$^-$ cells lacking FPN1 (Fig. 7, B [left] and E) were more pronounced.

Thus, forced Fpn1 expression clearly impairs the survival of *Salmonella* in PE-MΦ in a cell-autonomous manner.

Nos2 deficiency results in iron overload in mice

After these striking in vitro results, we investigated whether NOS2 might contribute to the regulation of iron homeostasis within mononuclear phagocytes in vivo. First, we assessed tissue iron distribution by Prussian blue staining. In line with the increased iron content measured in *Nos2*$^{-/-}$ macrophages (Fig. 1 A), we observed increased iron storage in spleens of *Nos2*$^{-/-}$ mice (Fig. 8, B and D). Iron storage was most prominent in the red pulp (rp), which is rich in mononuclear cells, whereas the white pulp (wp) of *Nos2*$^{-/-}$ mice showed hardly any iron accumulation (Fig. 8, B and D). Only very few and small iron foci were seen in (the red pulp of) *Nos2*$^{+/+}$ mice (Fig. 8, A and C). When measuring the iron content of the spleen and liver of uninfected mice, we observed that *Nos2*$^{-/-}$ mice had increased levels of tissue iron compared with *Nos2*$^{+/+}$ control mice (Fig. 8 E and not depicted). Notably, Nrf2 activation was reduced in nuclear extracts of spleens (Fig. 8 F) and livers (not depicted) from *Nos2*$^{-/-}$ mice relative to *Nos2*$^{+/+}$ controls.

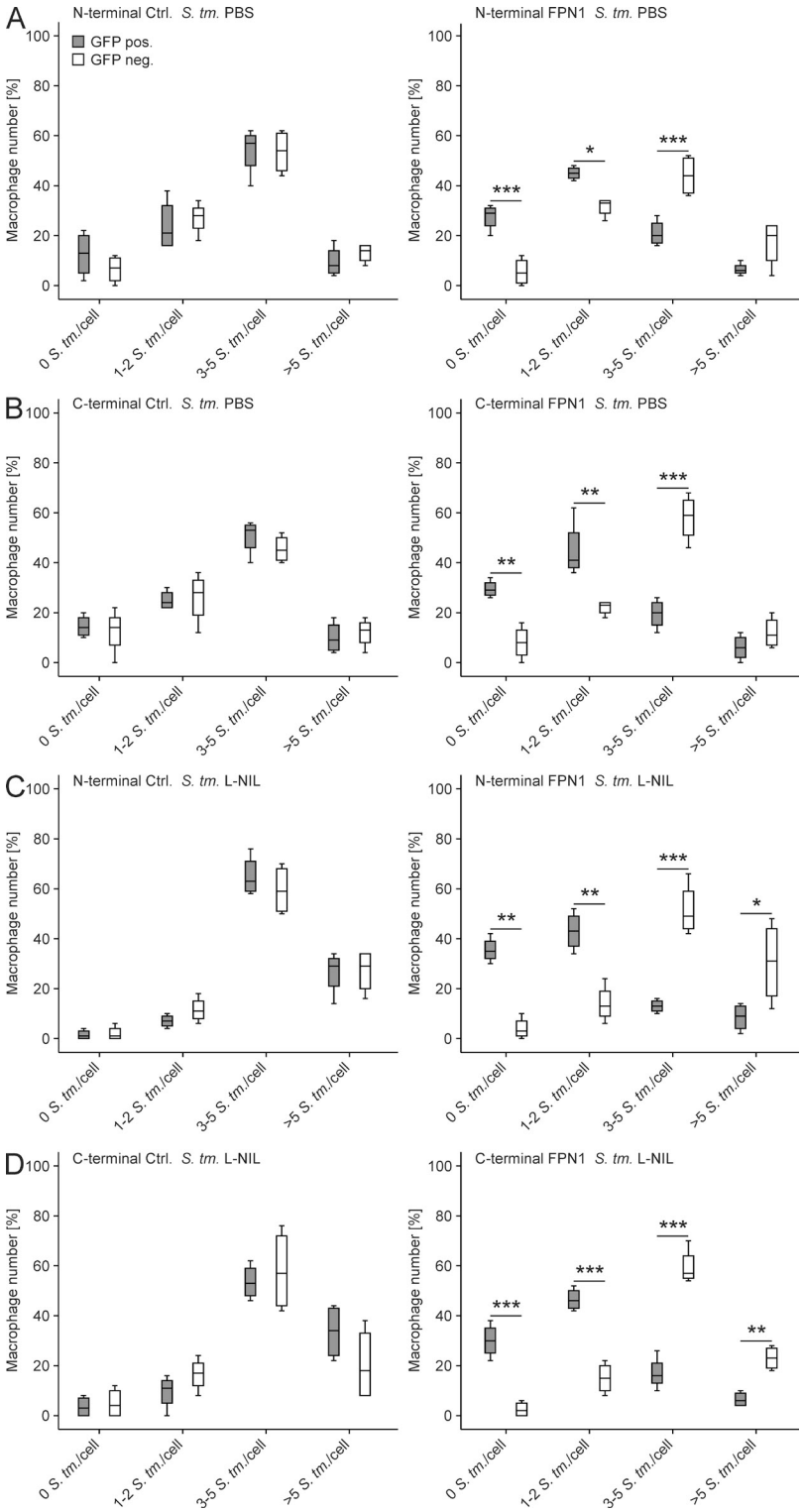

Figure 6. Overexpression of EmGFP-FPN1 constructs in *Nos2* wild-type and *Nos2*$^{-/-}$ PE-MΦ. (A–D) PE-MΦ were transiently transfected with empty EmGFP plasmids (left) or constructs coding for human FPN1 and EmGFP (right) linked to its N or C terminus, respectively. Subsequently, cells were infected with *S. typhimurium* and treated with PBS (A and B) or L-NIL (C and D) for 16 h. The number of intracellular bacteria was determined by immunofluorescence and is depicted as a function of GFP expression. For evaluation, PE-MΦ were grouped into 4 categories containing 0, 1–2, 3–5, or >5 bacteria per macrophage. Data were compared by ANOVA, followed by Bonferroni's correction ($n = 4$ independent experiments). *, $P < 0.05$; **, $P < 0.01$; ***, $P < 0.001$.

In livers, iron storage was more pronounced in Kupffer cells than in hepatocytes and the number of cells staining positive with Prussian blue was higher in *Nos2*$^{-/-}$ as compared with *Nos2*$^{+/+}$ livers (unpublished data). In line with the well-established NOS2 expression by liver parenchymal cells (Bogdan, 2001), the cellular iron content was also higher in isolated primary *Nos2*$^{-/-}$ as compared with *Nos2*$^{+/+}$ hepatocytes (Fig. 9 A).

Moreover, primary *Nos2*$^{-/-}$ hepatocytes expressed more hepcidin mRNA both under control conditions and in response to stimuli such as LPS, IL-6, and bone morphogenetic protein-6 (Bmp6). Conversely, exposure of NOS2$^{-/-}$ hepatocytes

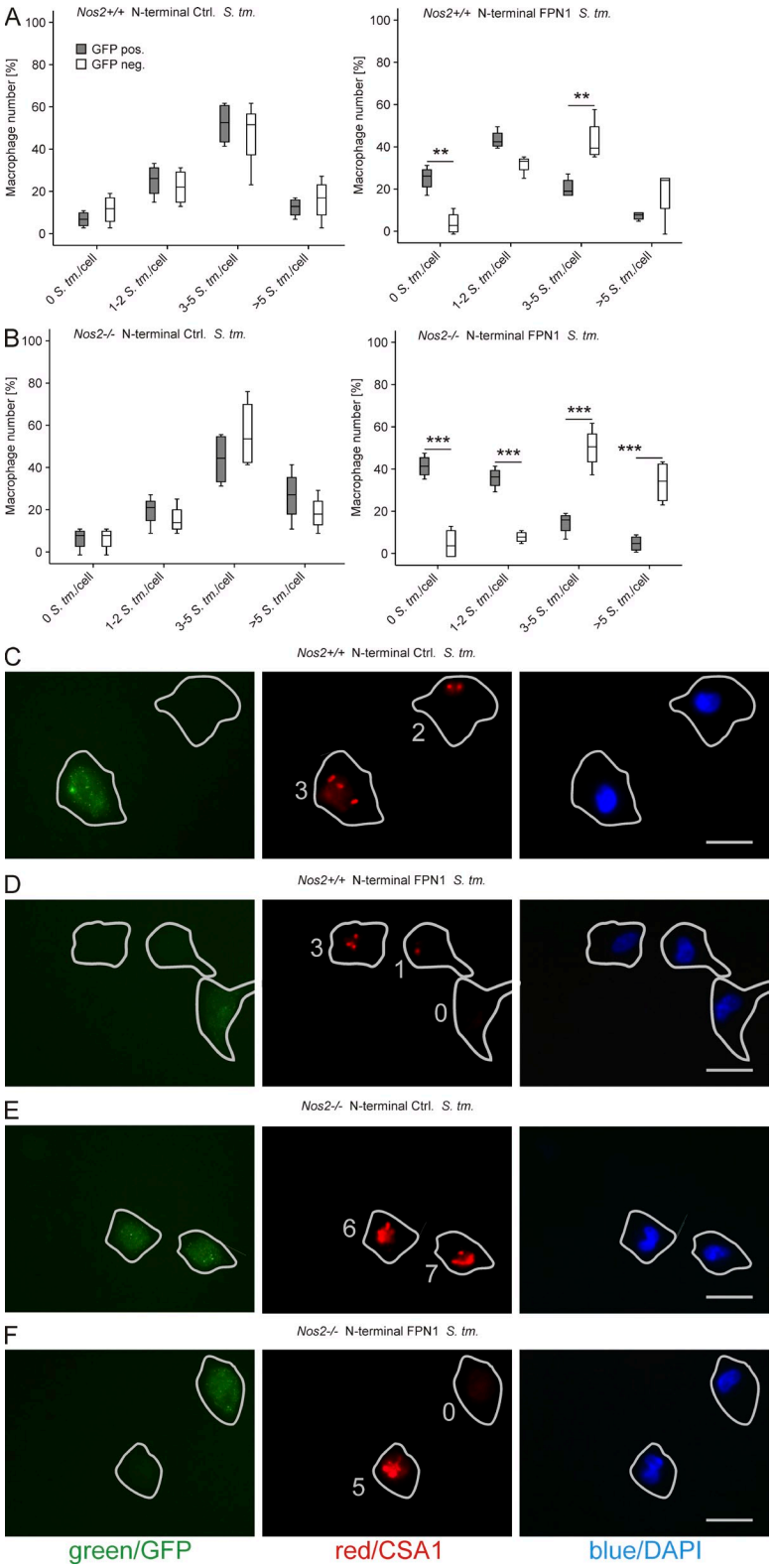

Figure 7. Immunofluorescence of EmGFP-FPN1–transfected and *Salmonella* infected *Nos2* wild-type and *Nos2*$^{-/-}$ PE-MΦ. (A and B) *Nos2* wild-type (A) and *Nos2*$^{-/-}$ (B) PE-MΦ were transfected with the N-terminal EmGFP-FPN1 construct (right) or empty plasmid (left). Subsequently, cells were infected with *S. typhimurium* for 16 h. The number of intracellular bacteria was determined by immunofluorescence and is depicted as a function of GFP expression as in Fig. 6 ($n = 4$ independent experiments). (C–F) Representative images acquired at 1,000× magnification are depicted. (left) GFP in green; (middle) CSA1/*S. typhimurium* in red; (right) DAPI/nuclei in blue. The cell membrane and the number of intracellular bacteria are indicated. Bars, 20 µm. (C and D) *Nos2* wild-type PE-MΦ were transiently transfected with empty EmGFP N-terminal plasmid (C) or a FPN1-EmGFP N-terminal construct (D), respectively. (E and F) *Nos2*$^{-/-}$ PE-MΦ were transiently transfected with empty EmGFP N-terminal plasmid (E) or a FPN1-EmGFP N-terminal construct (F), respectively. **, $P < 0.01$; ***, $P < 0.001$.

to the NO donor Nor5 rather reduced hepcidin mRNA formation in comparison to untreated control cells (Fig. 9 B). Thus, a lack of NOS2 is associated with an increased tissue iron load in vivo, which in the liver might cause an up-regulation of hepcidin.

NOS2-dependent iron restriction promotes host resistance to *Salmonella* infection in vivo

To see whether the NOS2- and Nrf2-dependent induction of Fpn1 is relevant for host defense in vivo, *Nos2*$^{+/+}$ and *Nos2*$^{-/-}$ mice were infected with 500 CFUs of *S. typhimurium*

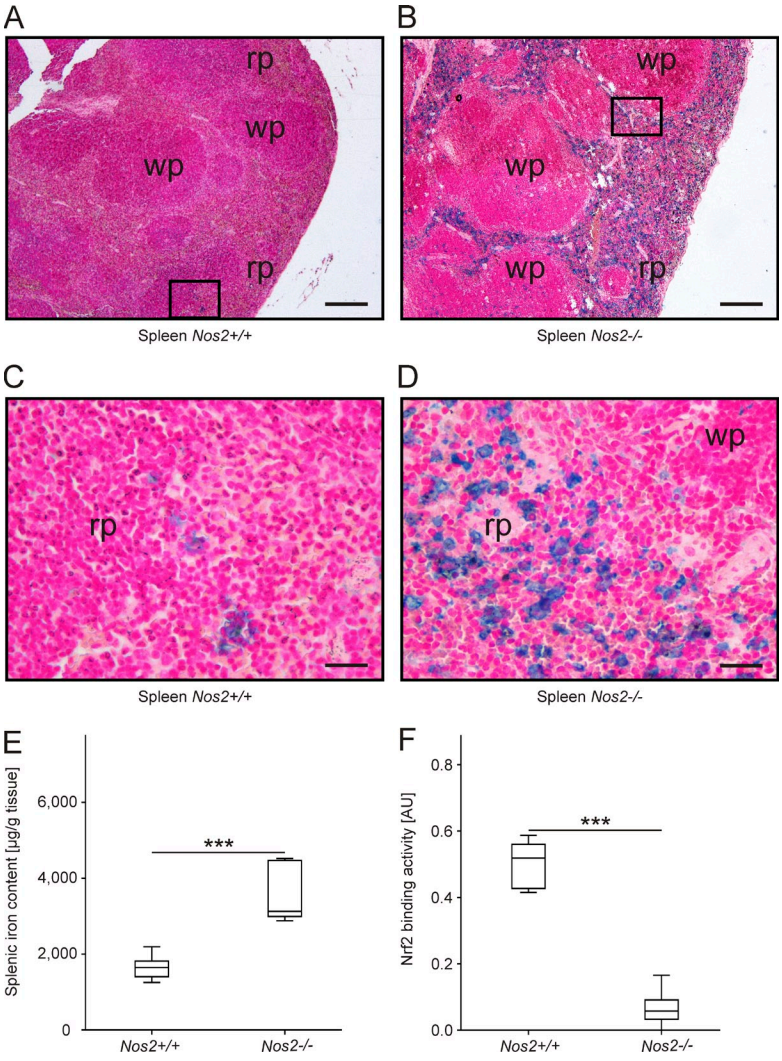

Figure 8. Splenic iron deposition and Nrf2-binding activity in *Nos2*$^{+/+}$ and *Nos2*$^{-/-}$ mice. (A–D) Prussian blue staining of spleen sections of *Nos2*$^{+/+}$ mice (A and C) and *Nos2*$^{-/-}$ mice (B and D). Insets in A and B (50×) represent areas shown at higher magnification (400×) in C and D. Scale bars: 200 µm (panels A and B), 50 µm (C and D). Red pulp (rp), white pulp (wp). (E) Tissue iron content in spleens of uninfected mice was determined by a colorimetric assay as described (Sonnweber et al., 2012; $n = 10$ individual mice per group). Data are depicted and were compared as in Fig. 1 A. (F) Nrf2-binding activity was determined in spleen nuclear extracts by a commercially available assay ($n = 6$ and 8 individual mice, respectively). ***, $P < 0.001$.

and analyzed after 24 and 72 h, respectively. At both time points, *Nos2*$^{-/-}$ mice contained significantly higher bacterial loads in spleens and livers than the respective wild-type controls (Fig. 10 A and not depicted).

In accordance with our results obtained with PE-MΦ, infection of *Nos2*$^{+/+}$ mice with *S. typhimurium* resulted in increased splenic Fpn1 protein levels, whereas in *Nos2*$^{-/-}$ mice Fpn1 remained at the level of uninfected mice (Fig. 10, B and C). Moreover, Nrf2-binding activity was induced after infection and was significantly higher in splenic nuclear extracts prepared from *Nos2*$^{+/+}$ mice as compared with *Nos2*$^{-/-}$ mice (Fig. 10 D).

Oral treatment of *Salmonella*-infected mice with DFX not only caused a significant reduction of the bacterial burden in

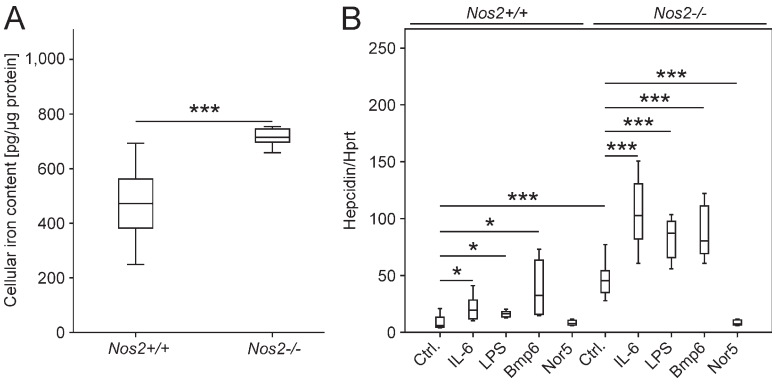

Figure 9. Iron content and hepcidin expression in *Nos2*$^{+/+}$ and *Nos2*$^{-/-}$ hepatocytes. (A) Cellular iron content of primary *Nos2*$^{+/+}$ and *Nos2*$^{-/-}$ hepatocytes was measured by atomic absorption spectrometry. Results were normalized for protein content and compared by Student's *t* test (cells isolated from $n = 12$ individual mice per group). (B) Primary *Nos2*$^{+/+}$ and *Nos2*$^{-/-}$ hepatocytes were isolated and stimulated with 100 ng/ml LPS, 10 ng/ml IL-6, 25 ng/ml Bmp-6, or 50 µM Nor5 for 6 h. Hepcidin mRNA levels were determined by qRT-PCR. Data, normalized for mRNA levels of the housekeeping gene Hprt, were compared by ANOVA using Bonferroni's correction ($n = 4$ independent experiments). *, $P < 0.05$; ***, $P < 0.001$.

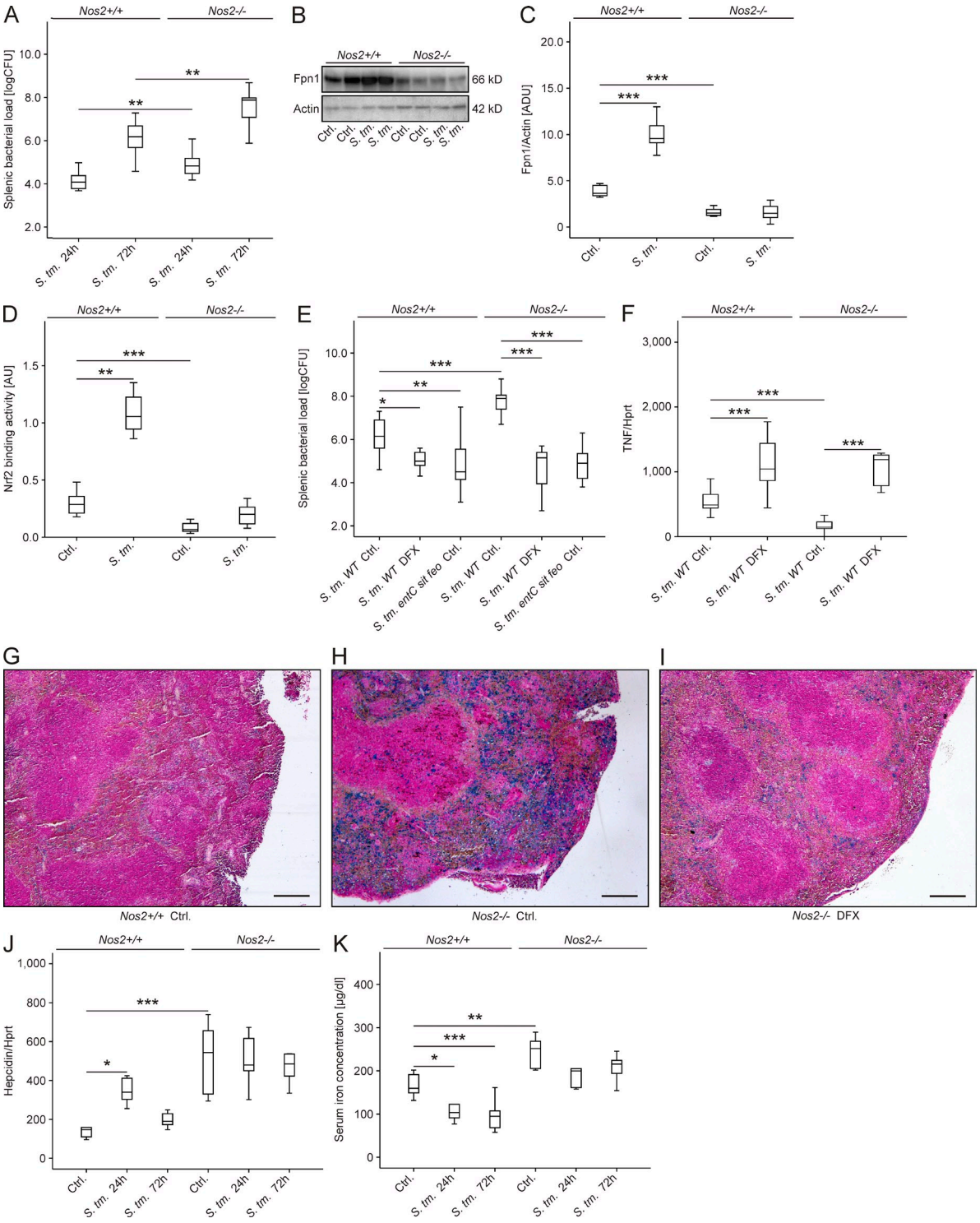

Figure 10. Splenic Fpn1 expression, Nrf2 activity, and DFX-treatment in systemic *S. typhimurium* infection. (A–D) *Nos2*$^{+/+}$ and *Nos2*$^{-/-}$ mice were infected i.p. with *S. typhimurium* (*S. tm.*) and euthanized after 24 or 72 h, respectively. (A) Bacterial loads in splenic lysates were determined and depicted as colony forming units after log transformation (logCFU; n = 10, 12, 5, and 11 mice, respectively). (B) Splenic samples of mice infected with *Salmonella* for 72 h were used for protein preparation and Fpn1 expression was analyzed by Western blotting. Actin is shown as loading control. Data from one of four independent experiments are depicted. (C) Fpn1 and actin levels were quantified by densitometric scanning of membranes. Data were compared by ANOVA using Bonferroni's correction (n = 8 independent experiments). (D) The binding affinity of Nrf2 in spleens of *Nos2*$^{+/+}$ and *Nos2*$^{-/-}$ mice was determined in nuclear extracts as described after infection with *Salmonella* for 72 h. Data were compared and depicted as in Fig. 2 A (n = 6, 8, 8, and 10 mice, respectively). (E–I) In independent experiments, *Nos2*$^{+/+}$ and *Nos2*$^{-/-}$ mice were i.p. infected with wild-type *S. typhimurium* (*S. tm. WT*) or

the spleen and liver of *Nos2*$^{+/+}$ and *Nos2*$^{-/-}$ mice, but also led to indistinguishable numbers of bacteria in the tissues of both genotypes (Fig. 10 E and not depicted). TNF, IL-12p35, and IFN-γ mRNA expression was higher in the spleens of *S. typhimurium*–infected *Nos2*$^{+/+}$ mice compared with *Nos2*$^{-/-}$ mice. DFX treatment caused an up-regulation of the mRNA expression of TNF, IL-12p35, and IFN-γ in the spleen of *Salmonella*-infected mice and abrogated the differences initially seen between *Nos2*$^{+/+}$ than *Nos2*$^{-/-}$ mice (Fig. 10 F and not depicted). In contrast, IL-23p19 and IL-17A mRNA levels remained unaffected by DFX treatment or *Nos2* genotype (unpublished data).

Prussian blue staining confirmed the efficacy of oral DFX-treatment in reducing splenic iron overload in *Nos2*$^{-/-}$ mice (Fig. 10, H vs. I). Supporting the concept that the increased susceptibility of *Nos2*$^{-/-}$ animals to *S. typhimurium* may result from increased microbial iron access, splenic and hepatic bacterial loads were comparable in *Nos2*$^{+/+}$ and *Nos2*$^{-/-}$ mice when infected with an *S. typhimurium entC sit feo* mutant that lacks three important iron acquisition systems (Fig. 10 E and not depicted).

Hepatic hepcidin mRNA levels were up-regulated in *Nos2*$^{+/+}$ mice in response to *Salmonella* infection, although a significant induction was only observed 24 h after the initiation of infection (Fig. 10 J). In *Nos2*$^{-/-}$ mice, in contrast, there were no further alterations of the higher basal hepcidin mRNA levels. After infection, *Nos2*$^{+/+}$ mice displayed a significant and prolonged reduction of serum iron levels, which was less evident in the absence of *Nos2* (Fig. 10 K).

DISCUSSION

In this study, we evaluated the putative role of NOS2 and its product NO as a mediator of host iron homeostasis and antimicrobial defense. We observed that NO induced the expression of Fpn1 in macrophages by activating the transcription factor Nrf2, thereby regulating cellular iron export under both resting conditions and in response to *Salmonella* infection. NO limits the ability of phagocytosed bacteria to obtain radiolabeled iron within infected macrophages, suggesting that NO-induced Fpn1 transcription resulted in iron deprivation of intracellular bacteria. Moreover, the addition of the iron chelator DFX to *Nos2*$^{-/-}$ macrophages reduced intracellular *Salmonella* numbers to levels seen in *Nos2*-expressing wild-type cells and restored the capacity of *Salmonella*-infected *Nos2*$^{-/-}$ macrophages to produce large amounts of TNF and IL-12. Thus, our findings suggest that the NOS2–Nrf2–Fpn1 axis is an important determinant of macrophage iron homeostasis and antimicrobial effector functions, which may counterbalance the hepcidin-induced Fpn1 degradation during infection with intracellular pathogens.

Iron, NO, and host defense

Several studies demonstrated the critical role of iron homeostasis in host defense (Byrd and Horwitz 1989; Weinberg, 2000; Collins 2003; Oexle et al., 2003; Schaible and Kaufmann, 2004; Schrettl et al., 2004; Nairz et al., 2010; Pagani et al., 2011; Johnson and Wessling-Resnick, 2012). During infections with intracellular pathogens, Fpn1-mediated iron export was a key component of the innate immune response (Chlosta et al., 2006; Nairz et al., 2007; Paradkar et al., 2008; Johnson et al., 2010; Mair et al., 2011). Hitherto, the molecular mechanism underlying Fpn1 induction in the presence of intracellular microbes has been unknown. Our observations show that NOS2, which has long been recognized as a central antimicrobial mechanism in a variety of infectious diseases (MacMicking et al., 1997; Bogdan, 2001), is a central mediator in the adaptation of iron metabolism after infection with the intracellular bacterium *S. typhimurium* (Mastroeni et al., 2000; Vazquez-Torres et al., 2000). In support of this conclusion, *Salmonella* residing within *Nos2*$^{-/-}$ macrophages was able to acquire significantly more iron in comparison to bacteria within wild-type macrophages. Thus, NO-mediated activation of Nrf2-dependent Fpn1 transcription appears to be a key component of innate immunity.

Because iron is an essential cofactor for enzymes involved in energy generation, we believe that reactive nitrogen species (RNS) and the NOS2–Fpn1–dependent iron restriction may act in concert to disrupt bacterial metabolism (Mastroeni et al., 2000; Vazquez-Torres et al., 2000). A recent report has shown that NO has multiple protein targets within bacterial metabolic pathways of *S. typhimurium* (Richardson et al., 2011). For instance, NO inactivated lipoamide-dependent oxidative decarboxylation reactions in *Salmonella* and thereby blocked the synthesis of methionine and lysine during nitrosative stress in vivo. Inhibition of the bacterial tricarboxylic acid cycle by NO also occurred by the targeting of iron–sulfur clusters within central enzymes and the transcriptional regulator FNR.

As a protective measure against RNS-induced damage, *S. typhimurium* expresses the flavohemoprotein Hmp to detoxify NO via a NsrR-regulated pathway (Crawford and Goldberg, 1998; Bang et al., 2006). Moreover, *Salmonella* Pathogenicity Island 2 reportedly inhibits trafficking of NOS2 to *Salmonella*-containing vacuoles to reduce nitrosative stress (Chakravortty et al., 2002).

an isogenic triple mutant, deficient in enterobactin synthesis, sitABCD-, and feo-mediated iron uptake (*S. tm. entC sit feo*). *Salmonella* wild-type–infected mice were randomized in two groups to receive either DFX dissolved in drinking water or the same volume of drinking water (Solv.). Bacterial loads (E; $n = 8, 13, 13, 7, 8,$ and 11 mice, respectively) in spleens were quantified and TNF (F; $n = 8, 13, 7,$ and 8 mice, respectively) expression were analyzed by qRT-PCR normalized to the housekeeping gene Hprt. (G-I) Prussian blue staining. Bar, 200 µm. (J) Hepatic hepcidin mRNA expression was determined by qRT-PCR and normalized for Hprt levels. Data were compared by ANOVA using Bonferroni's correction ($n = 9, 10, 12, 6, 5,$ and 11 mice, respectively). (K) Serum iron levels were colorimetrically measured and compared by ANOVA using Bonferroni's correction ($n = 9, 10, 12, 6, 5$ and 11 mice, respectively). *, $P < 0.05$; **, $P < 0.01$; ***, $P < 0.001$.

Apart from its direct antimicrobial actions, NOS2 exhibits diverse immunomodulatory effects on several types of immune cells (Bogdan, 2000, 2001). For instance, NOS2 is a co-stimulatory factor for the expression of IFN-γ mRNA during the innate phase of experimental cutaneous leishmaniasis (Diefenbach et al., 1998). NO may also affect IL-12 production by macrophages, although reports disagree on whether there is a positive, a negative, or no role of NOS2 in IL-12 secretion (Rothe et al., 1996; Huang et al., 1998; Lasarte et al., 1999; Mullins et al., 1999). Our present data demonstrate that macrophage functions in the setting of *Salmonella* infection are also critically dependent on NO, as Fpn1-mediated iron export was required for TNF, IL-12, and IFN-γ mRNA expression.

NO-induced Fpn1 transcription reduced cellular iron content. This may serve two purposes. First, it has long been recognized that iron inhibits *Nos2* transcription by reducing the binding affinity of NF-IL6 (Weiss et al., 1994; Dlaska and Weiss, 1999). Moreover, the reduced intracellular iron content of macrophages expressing the functional (i.e., resistant) variant of Nramp1-enhanced NOS2 transcription via IFN-regulatory factor-1 (IRF-1; Fritsche et al., 2003). The up-regulation of Fpn1-mediated iron export in response to NO may thus act as a feed-forward mechanism to allow sustained NO production despite NO-mediated activation of the IRP/IRE system, which would tend to increase iron uptake and intracellular iron storage (Drapier et al., 1993; Weiss et al., 1993; Wardrop et al., 2000; Wang et al., 2005). Our results with macrophages overexpressing functional human FPN1 variants show that increased RNS production in response to *Salmonella* infection is a result of macrophage iron depletion, as it could be inhibited by the addition of either iron sulfate or hepcidin. Our finding that FPN1 overexpression also promoted TNF and IL-12 production is in line with the idea that the cellular iron status is a central determinant of macrophage immunostimulatory and effector functions (De Domenico et al., 2010; Nairz et al., 2010; Pagani et al., 2011). Iron is known to impair Th1-type immune responses (Weiss et al., 1992; Mencacci et al., 1997; Oexle et al., 2003). Accordingly, $Nos2^{-/-}$ mice, which have increased splenic iron content, expressed lower levels of TNF, IL-12p35, and IFN-γ mRNA, but unaltered amounts of IL-17A mRNA in the spleen. This phenotype was completely reversed by DFX treatment. Thus, the Th1 pathway rather than Th17-mediated mechanisms were negatively modulated by a lack of NOS2-derived NO caused by an increased splenic iron content.

Additionally, NO has the potential to inhibit vital metabolic processes by directly targeting iron-sulfur cluster– and heme-containing centers of crucial enzymes (Drapier and Hibbs, 1988; Fang 2004; Henard and Vazquez-Torres, 2011). The induction of Fpn1 may thus aim at reducing cellular iron content to limit collateral damage by iron-catalyzed reactive oxygen species (ROS) and toxic congeners of NO and ROS (Stamler and Hausladen, 1998).

Mechanism of regulation of Fpn1 by NO

The role of NO for the regulation of the IRP/IRE system is well established (Hentze et al., 2004). Although NO activates IRP1 by disrupting its iron-sulfur cluster (Weiss et al., 1993), thus converting its activity from the enzymatic, cytoplasmic aconitase function to its IRE-binding function, IRP2 is activated when NO specifically inhibits its degradation through the proteasome (Wang et al., 2005). As cells lacking both IRP1 and IRP2 have increased Fpn1 protein levels but unchanged Fpn1 mRNA levels (Galy et al., 2008), it appears unlikely that the posttranslational control of Fpn1 expression via the IRP/IRE system substantially contributes to the NO-dependent regulation observed in our studies. Rather, NO-mediated activation of Nrf2 and subsequent transcriptional induction of Fpn1 expression appear to be responsible. In line with this mechanism, addition of the RNA polymerase II inhibitor actinomycin D abrogated the effects of NO on Fpn1 mRNA levels (unpublished data). Moreover, in our reporter studies, we used a Fpn1 promoter construct in which the IRE was specifically deleted (Marro et al., 2010). Despite the well-known interactions between NO and the IRP/IRE system, we did not observe differential IRP1 or IRP 2 protein content in the spleen of $Nos2^{-/-}$ and *Nos2* wild-type mice by means of Western blotting (unpublished data).

Nrf2 is an iron–sulfur cluster–containing basic leucine zipper transcription factor, which acts as a cellular stress sensor and initiates appropriate responses to oxidative stress. Nrf2 mediates both the constitutive and inducible expression of a variety of cytoprotective genes, including antioxidative enzymes and export proteins (Ishii et al., 2000). Recent studies have implicated Nrf2 as modifier of iron homeostasis. In macrophages, pharmacological activation of Nrf2 with sulforaphen was found to induce Fpn1 transcription (Harada et al., 2011). $Nrf2^{-/-}$ mice exhibit reduced iron content in the dental enamel but increased hepatic iron deposition. In a murine model of steatohepatitis, *Nrf2* deficiency was associated with reduced hepatic Fpn1 expression and, consequently, reduced hepatocellular iron export (Okada et al., 2012). Furthermore, renal Nrf2 is activated after injection with iron nitrilotriacetate, and $Nrf2^{-/-}$ mice display dramatically increased susceptibility to iron nitrilotriacetate-induced oxidative kidney damage caused by their inability to mount an appropriate nephroprotective response (Kanki et al., 2008; Tanaka et al., 2008). Thus, the Nrf2–Fpn1 pathway may be seen as a countermeasure to limit ongoing production of toxic radicals via iron-mediated Fenton chemistry.

Although the splenic iron distribution observed in $Nos2^{-/-}$ mice is similar to that seen in mice with myeloid-specific deletion of *Fpn1*, the immune phenotype is quite different between $Nos2^{-/-}$ mice with reduced Fpn1 levels and Fpn1-deficient $Fpn1^{LysM/LysM}$ mice (Zhang et al., 2011). We observed diminished production of TNF and IL-12p70 in *Salmonella*-infected $Nos2^{-/-}$ PE-MΦ that could be specifically reversed by overexpression of FPN1. In contrast, $Fpn1^{LysM/LysM}$ bone marrow–derived macrophages exhibit increased TNF and IL-6 secretion in response to LPS challenge that could be reversed by treatment with the iron chelator desferroxamine (DFO; Zhang et al., 2011).

In contrast to hepcidin, which causes ligand-induced lysosomal degradation of Fpn1, we identified NO as transcriptional Fpn1 inducer. It would thus be interesting to test the effects of NO donors in pathophysiological conditions associated with reduced Fpn1 activity such as ACD and cancer (Weiss and Goodnough, 2005; Nemeth and Ganz, 2006). We speculate that, by virtue of their capacity to up-regulate Fpn1, NO donors may counteract the functional iron deficiency underlying the pathogenesis of ACD.

We did not observe any significant effect of NO on hepcidin expression. Primary hepatocytes isolated from *Nos2*$^{-/-}$ mice responded appropriately to well-known hepcidin-inducing stimuli. In fact, *Nos2*$^{-/-}$ hepatocytes expressed elevated hepcidin levels under control conditions and showed up-regulation in response to IL-6, Bmp6, or LPS. In contrast, Nor5 did not affect basal hepcidin transcription in *Nos2*$^{+/+}$ hepatocytes, but NO treatment caused a significant decrease in hepcidin mRNA expression in *Nos2*$^{-/-}$ hepatocytes. We speculate that this regulation results from the induction of Fpn1 and the subsequent reduction of hepatocellular iron levels. Our data are compatible with the idea that the elevation of hepcidin observed in the absence of NOS2 in vitro and in vivo is secondary to iron overload rather than to a direct negative regulation of hepcidin gene expression by NO. In line with this assumption, we failed to observe a down-regulatory effect of NO on hepcidin mRNA expression (Fig. 1 F). Furthermore, the analysis of 6-wk-old mice revealed reduced Fpn1 levels in the spleen and liver of *Nos2*$^{-/-}$ mice as compared with *Nos2*$^{+/+}$ controls, whereas at this age, hepcidin mRNA levels in the liver of both mouse strains were indistinguishable (not depicted).

We observed that the hypoferremia in *Salmonella*-infected *Nos2*$^{+/+}$ mice was more pronounced and prolonged than in *Nos2*$^{-/-}$ mice, which presented with higher hepcidin expression than the infected wild-type animals. This suggests that additional, hepcidin-independent mechanisms may exist to mediate an appropriate reduction of serum iron levels in the setting of *Salmonella* infection. TNF has a well-established role in the hypoferremia of the acute-phase response and the control of cellular iron homeostasis (Ludwiczek et al., 2003; Laftah et al., 2006). Given its lower levels in *Nos2*$^{-/-}$ mice, TNF might also contribute to the observed differences between *Salmonella*-infected *Nos2*$^{+/+}$ and *Nos2*$^{-/-}$ mice.

We propose that in parallel to the hepcidin-mediated posttranslational down-regulation of Fpn1, NOS2/NO-dependent activation of Nrf2 and the subsequent transcriptional induction of Fpn1 controls cellular iron release and macrophage function. The NOS2–Nrf2–Fpn1 pathway is essential for macrophage responses to *S. typhimurium*, but presumably also for other intracellular pathogens. In line with our results, J774 macrophages overexpressing Fpn1 suppressed the intracellular growth of *Mycobacterium tuberculosis*. At the same time, however, the LPS-induced translation of NOS2 in these cells was impeded, an effect that remained mechanistically unexplained but reversible by IFN-γ (Johnson et al., 2010).

Therapeutic implications

Iron chelators may be useful for the treatment of infections with intracellular pathogens. Given the key role of iron for microbial pathogenicity, the iron chelator DFO has also been tested in models of *Salmonella* infection. Although its in vivo administration is associated with reduced survival of mice (Collins et al., 2002), this might be attributable to the ability of extracellular *Salmonella* to use ferrioxamines as an iron source (Kingsley et al., 1999). In contrast, DFO restricts intracellular *Salmonella* replication in vitro due to its ability to withhold iron from the microbe (Nairz et al., 2007). It is important to note that in our study, the water-soluble chelator DFX had beneficial effects on *Salmonella* infection both in vitro and in vivo. The difference between DFO and DFX may be related to diverse cellular penetration and a differential ability of these compounds to be used by *Salmonella* in a metal-bound state. In this context, it is worth noting that both DFX and deferiprone (DFP) have been used to limit the proliferation of *Chlamydia psittaci*, *Chlamydia pneumoniae*, and *Legionella pneumophila* in infected macrophages (Paradkar et al., 2008; Bellmann-Weiler et al., 2012). However, data on the potential use of oral iron chelators in the treatment of systemic infections remains scarce. DFX has been demonstrated to be effective in mucormycosis in animal models (Ibrahim et al., 2007). When mice subjected to chemotherapy-induced neutropenia or diabetic ketoacidosis were experimentally infected with *Rhizopus oryzae*, DFX-treatment reduced mortality, which was paralleled by the induction of Th1 cytokines TNF and IFN-γ in the spleens of DFX-treated mice. Our studies disclose the novel finding that oral application of DFX may beneficially affect the course of systemic infections with the intracellular bacterium *S. typhimurium*. However, whether this holds also true for other intracellular microbes during in vivo infection and whether these findings will translate into clinical benefits for infected humans, remains to be investigated. Nevertheless, DFX has proven clinical efficacy and safety in the treatment of secondary iron-overload in the setting of hemoglobinopathies (Cappellini et al., 2011).

In summary, the data presented here provide novel mechanistic insights into the antimicrobial role of NO in infection and into the regulation of macrophage iron homeostasis. NOS2-derived NO activates Nrf2, resulting in increased Fpn1 transcription, cellular iron export and limitation of iron availability for pathogens residing in macrophages. In addition, NOS2-mediated reduction of the macrophage iron content promotes a proinflammatory cytokine response. Our results imply that the NOS2-initiated iron export and its subsequent immunological and metabolic effects are important for the efficient control of infections with intracellular pathogens such as *S. typhimurium*.

MATERIALS AND METHODS

Cell isolation and culture. Thioglycolate-elicited PE-MΦ were harvested from C57BL/6J *Nos2*$^{+/+}$ and *Nos2*$^{-/-}$ mice and cultured as detailed elsewhere (Nairz et al., 2009b). Macrophages were incubated in DMEM and

treated with the NO donors Nor5 ((±)-2-((E)-4-Ethyl-3[(Z)-hydroxyimino]6-methyl-5-nitroheptenyl)-3-pyridinecarboxamide) or Gea5583 (1,2,3,4-Oxatriazolium, 3-(3-chloro-2-methylphenyl)-5(((cyanomethylamino) carbonyl)amino), hydroxide inner salt; 50 µM), both from Enzo Life Science, and dissolved in DMSO (final concentration 0.1%; Sigma-Aldrich) or the respective solvent control for the indicated time periods. For other experiments, the RNA polymerase II inhibitor actinomycin D (Sigma-Aldrich) was dissolved in DMSO and added at a concentration of 5 µg/ml. To determine mRNA half-life, cells were stimulated for 6 h, and then washed with fresh medium and subsequently incubated with actinomycin D or DMSO for different time periods.

RAW264.7 murine macrophage-like cells, originally isolated from *Nramp1*^{S} BALB/c mice, were stably transfected with the pHbβA-1-*neo* expression plasmid containing the full-length Nramp1 cDNA (Nramp1 resistant) or an antisense-Nramp1 construct (Nramp1 susceptible) and used as described previously (Nairz et al., 2009a).

Primary hepatocytes were isolated and cultured as described in detail elsewhere (Theurl et al., 2008b). Hepatocytes were incubated in Williams E medium and stimulated with phosphate buffered saline (PBS; obtained from PAA), 100 ng/ml LPS (from *Salmonella* Abortus equi; Sigma-Aldrich), 10 ng/ml recombinant IL-6 (R&D Systems), 25 ng/ml recombinant bone morphogenic protein (Bmp)-6 (Abcam), or a combination thereof for 6 or 24 h, respectively.

Intracellular iron concentrations in primary hepatocytes and macrophages were determined by atomic absorption as previously described (Theurl et al., 2008a). Blood samples were obtained from seven healthy individuals during routine vein puncture after written informed consent had been obtained in accordance with the Declaration of Helsinki. The study was approved by the MUI ethics committee at the Medical University of Innsbruck (approval no. AN3468-272/4.7). After isolation of white blood cells by Ficoll-Paque separation (Pharmacia), $CD14^{+}$ monocytes were freshly separated by magnetic sorting using specific MicroBeads (Miltenyi Biotec) after Ficoll-Paque separation (Pharmacia). The purity of the resulting cells suspension was tested by fluorescent-activated cell sorting analysis and was beyond 95% (Theurl et al., 2008b).

Salmonella infection in vitro. Before in vitro infection, macrophages were extensively washed with PBS and incubated in complete DMEM without antibiotics. Wild-type *S. typhimurium* strain ATCC 14028 was used for all experiments and grown under sterile conditions in LB broth (Sigma-Aldrich) to late-logarithmic phase. Macrophages were infected with *S. typhimurium* at a multiplicity of infection (MOI) of 10 for 24 h. Where appropriate, cells were subsequently treated with PBS, 600 µM L-NIL (L-N^{6}-[1-iminoethyl]-lysine.2HCl; purchased from Enzo Life Sciences), 50 µM deferasirox (DFX; from Novartis), 50 µM $FeSO_4$ (Sigma-Aldrich) or 1 µM synthetic murine hepcidin (PeptaNova). For experiments in which human FPN1 variants were overexpressed, and 1 µM synthetic human hepcidin (PeptaNova) was used. To determine intracellular bacterial loads, infected cells were harvested in 0.1% sodium deoxycholic acid (Sigma-Aldrich) as previously described (Nairz et al., 2009b).

Salmonella infection in vivo. C57BL/6J type mice (*Nos2*$^{+/+}$) and *Nos2*$^{-/-}$ mice (Laubach et al., 1995) that were backcrossed onto a C57BL/6J background for at least 11 generations (JAX stock number 2609) were obtained at the age of 4–6 wk from The Jackson Laboratories via the Charles River Breeding Laboratories. Congenic mice were housed in neighboring cages under specific pathogen–free conditions at the central animal facility of the Medical University of Innsbruck or at the Franz Penzoldt Center for Animal Research of the Universitätsklinikum Erlangen. All animal experiments were performed according to the guidelines of the Medical University of Innsbruck based on the Austrian Animal Testing Act of 1988. All animal experiment protocols were approved by the MUI Animal ethics committee and the Austrian Ministry for Science and Education (approval no. BMWF-66.011/0151-II/3b/2011). Unless otherwise indicated, male mice were used at 18–20 wk of age and infected i.p. with 500 CFU of *S. typhimurium* diluted in 200 µl PBS. Unless otherwise specified, *S. typhimurium* wild-type strain ATCC 14028s was used for experiments. In some experiments, its isogenic triple mutant derivative *entC*::*aph sit*::*bla feo*::*Tn*10 (Kan^{r} Ap^{r} Tet^{r}) was used. This mutant strain was constructed and grown as previously described (Crouch et al., 2008) and used as detailed above. Where indicated, mice received DFX ad libitum via the oral route by dissolving 500 mg DFX in 1,000 ml drinking water. The bacterial load of organs was determined by plating serial dilutions of organ homogenates on LB agar (Sigma-Aldrich) under sterile conditions and the number of bacteria was calculated per gram of tissue as previously described (Nairz et al., 2011).

RNA extraction and quantitative real-time PCR. Total RNA was prepared and mRNA expression quantified by quantitative RT-PCR after reverse transcription exactly as described (Nairz et al., 2009b).

Western blot analysis. Protein extraction and Western blotting were performed exactly as described (Theurl et al., 2006) using a rabbit Fpn1 antibody (1:400; Eurogentec), a rabbit actin antibody (1:1,000; Sigma-Aldrich), and appropriate HRP-conjugated secondary antibodies (1:1,000; Dako).

Immunocytochemistry. PE-MΦ were seeded on glass slides, transfected as described below, and subsequently infected for 16 h. After fixation with ice-cold methanol for 15 min on ice, cells were rinsed twice with PBS containing 0.1% Tween-20 and sequentially incubated with antibodies as follows: a chicken GFP antibody (1:1000; Invitrogen), a goat CSA1 (for *Salmonella* common structural antigen) antibody (1:1,000; KPL), and appropriate fluorochrome-conjugated secondary antibodies, i.e., rabbit anti–chicken Alexa Fluor 488 (green; 1:1,000; Dianova) and donkey anti–goat Alexa Fluor 594 (red; 1:1,000; Invitrogen). For microscopic analysis, the cells were covered into Fluorescent Mounting Medium (Dako) containing DAPI and analyzed under the Axioskop 2 microscope (Carl Zeiss). Acquisition was done using the AxioCam MRc 5 camera, a 100×/1.25 objective, and the AxioVision imaging software version 4.0 (Carl Zeiss).

Transcription factor assay. Nuclear protein extracts were prepared with the Nuclear and Cytoplasmic Extraction Reagent (Thermo Fisher Scientific). Nrf2-binding activity of nuclear extracts was assessed with a commercially available colorimetric transcription factor assay kit exactly according to the manufacturer's instructions (Active Motif).

Plasmids and transient transfection. To generate the 8-kbΔIRE-Fpn1 construct, a fragment of the mouse Fpn1 promoter containing the 5′-UTR and 8,071 bp upstream of the transcription start site was cloned into the pGL3 luciferase reporter gene vector (Promega). A corresponding variant lacking the Nrf2-binding site at position −7007/−7016 was constructed by site-specific mutagenesis as previously described (Marro et al., 2010). Plasmids were kindly provided by S. Marro, E. Messana, and S. Altamura (University of Heidelberg, Heidelberg, Germany; and Molecular Biotechnology Center, University of Torino, Torino, Italy).

The 1.6-kb full-length murine *Nos2* promoter was cloned into the pGL3 luciferase reporter gene vector as previously described (Dlaska and Weiss, 1999). Promoter activity was determined by the Dual Luciferase system (Promega) according to the manufacturer's instructions. Firefly luciferase activity was corrected by co-transfection of cells with the constitutively expressed Renilla luciferase vector pRL-SV40.

Mouse Nrf2 was cloned into the p-cDNA3.1 expression plasmid as previously specified (Song et al., 2009), and the construct was generously provided by M.-Y. Song, H.-S. So, and B.-H. Park (Medical School, Chonbuk National University, Jeonju, Jeonbuk, South Korea). Human FPN1 and the N144H and A77D FPN1 mutants, respectively, were cloned into the p-cDNA3.1/c-Myc expression vector as described previously (Drakesmith et al., 2005; L. Schimanski and H. Drakesmith, Weatherall Institute of Molecular Medicine, Oxford, England, UK). Transient transfections of primary PE-MΦ were performed by means of lipofection using Lipofectamine (Promega).

For immunocytochemistry, we used EmGFP N- or C-terminally tagged human FPN1 expression clones, provided by H. Zoller (Department of Internal Medicine II, Medical University of Innsbruck, Austria), as previously described (Mayr et al., 2011). The FPN1 open reading sequence was transferred into Vivid Colors pcDNA 6.2/EmGFP-DEST vectors to create EmGFP FPN1 expression clones. As control vectors, we used Vivid Colors pcDNA 6.2 EmGFP/CAT (chloramphenicol acetyltransferase) plasmids. Efficacy of transfections was at least 70–85%.

Detection of cytokines and reactive species. Determination of cytokines in culture supernatants was performed with ELISA kits for TNF and IL-12p70 (BD). Determination of nitrite, the stable oxidation product of NO, was performed with the Griess-Ilosvay's nitrite reagent (Merck) as previously described (Nairz et al., 2008).

Quantification of macrophage iron export and bacterial iron acquisition. For macrophage iron export assays, cells were treated and infected with *S. typhimurium* as detailed above and iron export was determined with 5 μM ^{59}Fe-citrate exactly as previously described (Nairz et al., 2009a). In parallel to each iron release study, a Trypan blue exclusion assay was performed to ensure that neither treatment interfered with the macrophage integrity and viability. For the determination of iron acquisition by intramacrophage *S. typhimurium* we used a protocol as described (Nairz et al., 2007).

Statistical analysis. Statistical analysis was performed using a SPSS statistical package. We determined significance by unpaired two-tailed Student's *t* test to assess data, when only two groups were compared. ANOVA combined with Bonferroni correction was used for all other experiments. Unless otherwise specified, data are depicted as lower quartile, median, and upper quartile (boxes), and minimum/maximum ranges. For the comparison of organ bacterial loads, data were log-transformed before Student's *t* test or analysis of variance. Individual values and means of log-transformed values are depicted. Generally, p-values less than 0.05 were considered significant in any test.

The authors are grateful to Nadja Baumgartner, Sylvia Berger, Ines Brosch, Sabine Engl, and Markus Seifert for excellent technical support.

The authors are indebted to Mrs. Lisa Schimanski and Drs. Sandro Altamura, Howard C. Barton, Hal Drakesmith, Samuele Marro, Erika Messana, Byung-Hyun Park, Hong-Soeb So, Mi-Young Song, and Heinz Zoller for providing plasmids and cell lines.

This work was supported by grants from the Austrian Research Fund (FWF; project TRP-188 to G. Weiss), the Medical University of Innsbruck (START program; to M. Nairz), and the German Research Foundation (DFG; SFB643 to U. Schleicher and C. Bogdan), by the Interdisciplinary Center for Clinical Research Erlangen (project grant A49 to U. Schleicher and C. Bogdan), and by the Verein zur Förderung von Forschung und Weiterbildung in Infektiologie und Immunologie an der Medizinischen Universität Innsbruck. F. Fang is supported by the National Institutes of Health (AI39557).

The authors declare no competing financial interests.

Submitted: 29 August 2012
Accepted: 11 March 2013

REFERENCES

Abboud, S., and D.J. Haile. 2000. A novel mammalian iron-regulated protein involved in intracellular iron metabolism. *J. Biol. Chem.* 275:19906–19912. http://dx.doi.org/10.1074/jbc.M000713200

Armitage, A.E., L.A. Eddowes, U. Gileadi, S. Cole, N. Spottiswoode, T.A. Selvakumar, L.P. Ho, A.R. Townsend, and H. Drakesmith. 2011. Hepcidin regulation by innate immune and infectious stimuli. *Blood.* 118:4129–4139. http://dx.doi.org/10.1182/blood-2011-04-351957

Bang, I.S., L. Liu, A. Vazquez-Torres, M.L. Crouch, J.S. Stamler, and F.C. Fang. 2006. Maintenance of nitric oxide and redox homeostasis by the salmonella flavohemoglobin hmp. *J. Biol. Chem.* 281:28039–28047. http://dx.doi.org/10.1074/jbc.M605174200

Bellmann-Weiler, R., A. Schroll, S. Engl, M. Nairz, H. Talasz, M. Seifert, and G. Weiss. 2012. Neutrophil gelatinase-associated lipocalin and interleukin-10 regulate intramacrophage *Chlamydia pneumoniae* replication by modulating intracellular iron homeostasis. *Immunobiology.* 12:535–539. http://dx.doi.org/10.1016/j.imbio.2012.11.004.

Bogdan, C. 2001. Nitric oxide and the immune response. *Nat. Immunol.* 2:907–916. http://dx.doi.org/10.1038/ni1001-907

Bogdan, C. 2011. Regulation of lymphocytes by nitric oxide. *Methods Mol. Biol.* 677:375–393. http://dx.doi.org/10.1007/978-1-60761-869-0_24

Bogdan, C., M. Röllinghoff, and A. Diefenbach. 2000. The role of nitric oxide in innate immunity. *Immunol. Rev.* 173:17–26. http://dx.doi.org/10.1034/j.1600-065X.2000.917307.x

Byrd, T.F., and M.A. Horwitz. 1989. Interferon gamma-activated human monocytes downregulate transferrin receptors and inhibit the intracellular multiplication of *Legionella pneumophila* by limiting the availability of iron. *J. Clin. Invest.* 83:1457–1465. http://dx.doi.org/10.1172/JCI114038

Cappellini, M.D., M. Bejaoui, L. Agaoglu, D. Canatan, M. Capra, A. Cohen, G. Drelichman, M. Economou, S. Fattoum, A. Kattamis, et al. 2011. Iron chelation with deferasirox in adult and pediatric patients with thalassemia major: efficacy and safety during 5 years' follow-up. *Blood.* 118:884–893. http://dx.doi.org/10.1182/blood-2010-11-316646

Chakravortty, D., I. Hansen-Wester, and M. Hensel. 2002. *Salmonella* pathogenicity island 2 mediates protection of intracellular Salmonella from reactive nitrogen intermediates. *J. Exp. Med.* 195:1155–1166. http://dx.doi.org/10.1084/jem.20011547

Chlosta, S., D.S. Fishman, L. Harrington, E.E. Johnson, M.D. Knutson, M. Wessling-Resnick, and B.J. Cherayil. 2006. The iron efflux protein ferroportin regulates the intracellular growth of *Salmonella enterica*. *Infect. Immun.* 74:3065–3067. http://dx.doi.org/10.1128/IAI.74.5.3065-3067.2006

Collins, H.L. 2003. The role of iron in infections with intracellular bacteria. *Immunol. Lett.* 85:193–195. http://dx.doi.org/10.1016/S0165-2478(02)00229-8

Collins, H.L., S.H. Kaufmann, and U.E. Schaible. 2002. Iron chelation via deferoxamine exacerbates experimental salmonellosis via inhibition of the nicotinamide adenine dinucleotide phosphate oxidase-dependent respiratory burst. *J. Immunol.* 168:3458–3463.

Crawford, M.J., and D.E. Goldberg. 1998. Role for the *Salmonella* flavohemoglobin in protection from nitric oxide. *J. Biol. Chem.* 273:12543–12547. http://dx.doi.org/10.1074/jbc.273.20.12543

Crouch, M.L., M. Castor, J.E. Karlinsey, T. Kalhorn, and F.C. Fang. 2008. Biosynthesis and IroC-dependent export of the siderophore salmochelin are essential for virulence of Salmonella enterica serovar Typhimurium. *Mol. Microbiol.* 67:971–983. http://dx.doi.org/10.1111/j.1365-2958.2007.06089.x

De Domenico, I., T.Y. Zhang, C.L. Koening, R.W. Branch, N. London, E. Lo, R.A. Daynes, J.P. Kushner, D. Li, D.M. Ward, and J. Kaplan. 2010. Hepcidin mediates transcriptional changes that modulate acute cytokine-induced inflammatory responses in mice. *J. Clin. Invest.* 120:2395–2405. http://dx.doi.org/10.1172/JCI42011

Diefenbach, A., H. Schindler, N. Donhauser, E. Lorenz, T. Laskay, J. MacMicking, M. Röllinghoff, I. Gresser, and C. Bogdan. 1998. Type 1 interferon (IFNalpha/beta) and type 2 nitric oxide synthase regulate the innate immune response to a protozoan parasite. *Immunity.* 8:77–87. http://dx.doi.org/10.1016/S1074-7613(00)80460-4

Dlaska, M., and G. Weiss. 1999. Central role of transcription factor NF-IL6 for cytokine and iron-mediated regulation of murine inducible nitric oxide synthase expression. *J. Immunol.* 162:6171–6177.

Donovan, A., A. Brownlie, Y. Zhou, J. Shepard, S.J. Pratt, J. Moynihan, B.H. Paw, A. Drejer, B. Barut, A. Zapata, et al. 2000. Positional cloning of zebrafish ferroportin1 identifies a conserved vertebrate iron exporter. *Nature.* 403:776–781. http://dx.doi.org/10.1038/35001596

Drakesmith, H., L.M. Schimanski, E. Ormerod, A.T. Merryweather-Clarke, V. Viprakasit, J.P. Edwards, E. Sweetland, J.M. Bastin, D. Cowley, Y. Chinthammitr, et al. 2005. Resistance to hepcidin is conferred by

hemochromatosis-associated mutations of ferroportin. *Blood*. 106:1092–1097. http://dx.doi.org/10.1182/blood-2005-02-0561

Drapier, J.C., and J.B. Hibbs Jr. 1988. Differentiation of murine macrophages to express nonspecific cytotoxicity for tumor cells results in L-arginine-dependent inhibition of mitochondrial iron-sulfur enzymes in the macrophage effector cells. *J. Immunol.* 140:2829–2838.

Drapier, J.C., H. Hirling, J. Wietzerbin, P. Kaldy, and L.C. Kühn. 1993. Biosynthesis of nitric oxide activates iron regulatory factor in macrophages. *EMBO J.* 12:3643–3649.

Fang, F.C. 2004. Antimicrobial reactive oxygen and nitrogen species: concepts and controversies. *Nat. Rev. Microbiol.* 2:820–832. http://dx.doi.org/10.1038/nrmicro1004

Fritsche, G., M. Dlaska, H. Barton, I. Theurl, K. Garimorth, and G. Weiss. 2003. Nramp1 functionality increases inducible nitric oxide synthase transcription via stimulation of IFN regulatory factor 1 expression. *J. Immunol.* 171:1994–1998.

Galy, B., D. Ferring-Appel, S. Kaden, H.J. Gröne, and M.W. Hentze. 2008. Iron regulatory proteins are essential for intestinal function and control key iron absorption molecules in the duodenum. *Cell Metab.* 7:79–85. http://dx.doi.org/10.1016/j.cmet.2007.10.006

Ganz, T. 2009. Iron in innate immunity: starve the invaders. *Curr. Opin. Immunol.* 21:63–67. http://dx.doi.org/10.1016/j.coi.2009.01.011

Harada, N., M. Kanayama, A. Maruyama, A. Yoshida, K. Tazumi, T. Hosoya, J. Mimura, T. Toki, J.M. Maher, M. Yamamoto, and K. Itoh. 2011. Nrf2 regulates ferroportin 1-mediated iron efflux and counteracts lipopolysaccharide-induced ferroportin 1 mRNA suppression in macrophages. *Arch. Biochem. Biophys.* 508:101–109. http://dx.doi.org/10.1016/j.abb.2011.02.001

Henard, C.A., and A. Vazquez-Torres. 2011. Nitric oxide and salmonella pathogenesis. Front. Microbiol. 2:84–94. http://dx.doi.org/10.3389/fmicb.2011.00084

Hentze, M.W., M.U. Muckenthaler, and N.C. Andrews. 2004. Balancing acts: molecular control of mammalian iron metabolism. *Cell*. 117:285–297. http://dx.doi.org/10.1016/S0092-8674(04)00343-5

Huang, F.P., W. Niedbala, X.Q. Wei, D. Xu, G.J. Feng, J.H. Robinson, C. Lam, and F.Y. Liew. 1998. Nitric oxide regulates Th1 cell development through the inhibition of IL-12 synthesis by macrophages. *Eur. J. Immunol.* 28:4062–4070.

Ibrahim, A.S., T. Gebermariam, Y. Fu, L. Lin, M.I. Husseiny, S.W. French, J. Schwartz, C.D. Skory, J.E. Edwards Jr., and B.J. Spellberg. 2007. The iron chelator deferasirox protects mice from mucormycosis through iron starvation. *J. Clin. Invest.* 117:2649–2657. http://dx.doi.org/10.1172/JCI32338

Ishii, T., K. Itoh, S. Takahashi, H. Sato, T. Yanagawa, Y. Katoh, S. Bannai, and M. Yamamoto. 2000. Transcription factor Nrf2 coordinately regulates a group of oxidative stress-inducible genes in macrophages. *J. Biol. Chem.* 275:16023–16029. http://dx.doi.org/10.1074/jbc.275.21.16023

Johnson, E.E., and M. Wessling-Resnick. 2012. Iron metabolism and the innate immune response to infection. *Microbes Infect.* 14:207–216. http://dx.doi.org/10.1016/j.micinf.2011.10.001

Johnson, E.E., A. Sandgren, B.J. Cherayil, M. Murray, and M. Wessling-Resnick. 2010. Role of ferroportin in macrophage-mediated immunity. *Infect. Immun.* 78:5099–5106. http://dx.doi.org/10.1128/IAI.00498-10

Kanki, K., T. Umemura, Y. Kitamura, Y. Ishii, Y. Kuroiwa, Y. Kodama, K. Itoh, M. Yamamoto, A. Nishikawa, and M. Hirose. 2008. A possible role of nrf2 in prevention of renal oxidative damage by ferric nitrilotriacetate. *Toxicol. Pathol.* 36:353–361. http://dx.doi.org/10.1177/0192623307311401

Kemna, E.H., P. Pickkers, E. Nemeth, H. van der Hoeven, and D. Swinkels. 2005. Time-course analysis of hepcidin, serum iron, and plasma cytokine levels in humans injected with LPS. *Blood*. 106:1864–1866. http://dx.doi.org/10.1182/blood-2005-03-1159

Kingsley, R.A., R. Reissbrodt, W. Rabsch, J.M. Ketley, R.M. Tsolis, P. Everest, G. Dougan, A.J. Bäumler, M. Roberts, and P.H. Williams. 1999. Ferrioxamine-mediated Iron(III) utilization by *Salmonella enterica*. *Appl. Environ. Microbiol.* 65:1610–1618.

Laftah, A.H., N. Sharma, M.J. Brookes, A.T. McKie, R.J. Simpson, T.H. Iqbal, and C. Tselepis. 2006. Tumour necrosis factor alpha causes hypoferraemia and reduced intestinal iron absorption in mice. *Biochem. J.* 397:61–67. http://dx.doi.org/10.1042/BJ20060215

Lasarte, J.J., F.J. Corrales, N. Casares, A. López-Díaz de Cerio, C. Qian, X. Xie, F. Borrás-Cuesta, and J. Prieto. 1999. Different doses of adenoviral vector expressing IL-12 enhance or depress the immune response to a coadministered antigen: the role of nitric oxide. *J. Immunol.* 162:5270–5277.

Laubach, V.E., E.G. Shesely, O. Smithies, and P.A. Sherman. 1995. Mice lacking inducible nitric oxide synthase are not resistant to lipopolysaccharide-induced death. *Proc. Natl. Acad. Sci. USA*. 92:10688–10692. http://dx.doi.org/10.1073/pnas.92.23.10688

Ludwiczek, S., E. Aigner, I. Theurl, and G. Weiss. 2003. Cytokine-mediated regulation of iron transport in human monocytic cells. *Blood*. 101:4148–4154. http://dx.doi.org/10.1182/blood-2002-08-2459

MacMicking, J., Q.W. Xie, and C. Nathan. 1997. Nitric oxide and macrophage function. *Annu. Rev. Immunol.* 15:323–350. http://dx.doi.org/10.1146/annurev.immunol.15.1.323

Mair, S.M., M. Nairz, R. Bellmann-Weiler, T. Muehlbacher, A. Schroll, I. Theurl, P.L. Moser, H. Talasz, F.C. Fang, and G. Weiss. 2011. Nifedipine affects the course of Salmonella enterica serovar Typhimurium infection by modulating macrophage iron homeostasis. *J. Infect. Dis.* 204:685–694. http://dx.doi.org/10.1093/infdis/jir395

Marro, S., D. Chiabrando, E. Messana, J. Stolte, E. Turco, E. Tolosano, and M.U. Muckenthaler. 2010. Heme controls ferroportin1 (FPN1) transcription involving Bach1, Nrf2 and a MARE/ARE sequence motif at position -7007 of the FPN1 promoter. *Haematologica.* 95:1261–1268. http://dx.doi.org/10.3324/haematol.2009.020123

Mastroeni, P., A. Vazquez-Torres, F.C. Fang, Y. Xu, S. Khan, C.E. Hormaeche, and G. Dougan. 2000. Antimicrobial actions of the NADPH phagocyte oxidase and inducible nitric oxide synthase in experimental salmonellosis. II. Effects on microbial proliferation and host survival in vivo. *J. Exp. Med.* 192:237–248. http://dx.doi.org/10.1084/jem.192.2.237

Mayr, R., W.J. Griffiths, M. Hermann, I. McFarlane, D.J. Halsall, A. Finkenstedt, A. Douds, S.E. Davies, A.R. Janecke, W. Vogel, et al. 2011. Identification of mutations in SLC40A1 that affect ferroportin function and phenotype of human ferroportin iron overload. *Gastroenterology*. 140:2056–2063: 2063: e1. http://dx.doi.org/10.1053/j.gastro.2011.02.064

McKie, A.T., P. Marciani, A. Rolfs, K. Brennan, K. Wehr, D. Barrow, S. Miret, A. Bomford, T.J. Peters, F. Farzaneh, et al. 2000. A novel duodenal iron-regulated transporter, IREG1, implicated in the basolateral transfer of iron to the circulation. *Mol. Cell.* 5:299–309. http://dx.doi.org/10.1016/S1097-2765(00)80425-6

Melillo, G., L.S. Taylor, A. Brooks, T. Musso, G.W. Cox, and L. Varesio. 1997. Functional requirement of the hypoxia-responsive element in the activation of the inducible nitric oxide synthase promoter by the iron chelator desferrioxamine. *J. Biol. Chem.* 272:12236–12243.

Mencacci, A., E. Cenci, J.R. Boelaert, P. Bucci, P. Mosci, C. Fè d'Ostiani, F. Bistoni, and L. Romani. 1997. Iron overload alters innate and T helper cell responses to Candida albicans in mice. *J. Infect. Dis.* 175:1467–1476. http://dx.doi.org/10.1086/516481

Mullins, D.W., C.J. Burger, and K.D. Elgert. 1999. Paclitaxel enhances macrophage IL-12 production in tumor-bearing hosts through nitric oxide. *J. Immunol.* 162:6811–6818.

Nairz, M., I. Theurl, S. Ludwiczek, M. Theurl, S.M. Mair, G. Fritsche, and G. Weiss. 2007. The co-ordinated regulation of iron homeostasis in murine macrophages limits the availability of iron for intracellular Salmonella typhimurium. *Cell. Microbiol.* 9:2126–2140. http://dx.doi.org/10.1111/j.1462-5822.2007.00942.x

Nairz, M., G. Fritsche, P. Brunner, H. Talasz, K. Hantke, and G. Weiss. 2008. Interferon-gamma limits the availability of iron for intramacrophage Salmonella typhimurium. *Eur. J. Immunol.* 38:1923–1936. http://dx.doi.org/10.1002/eji.200738056

Nairz, M., G. Fritsche, M.L. Crouch, H.C. Barton, F.C. Fang, and G. Weiss. 2009a. Slc11a1 limits intracellular growth of Salmonella enterica sv. Typhimurium by promoting macrophage immune effector functions and impairing bacterial iron acquisition. *Cell. Microbiol.* 11:1365–1381. http://dx.doi.org/10.1111/j.1462-5822.2009.01337.x

Nairz, M., I. Theurl, A. Schroll, M. Theurl, G. Fritsche, E. Lindner, M. Seifert, M.L. Crouch, K. Hantke, S. Akira, et al. 2009b. Absence of functional Hfe protects mice from invasive Salmonella enterica serovar Typhimurium infection via induction of lipocalin-2. *Blood*. 114:3642–3651. http://dx.doi.org/10.1182/blood-2009-05-223354

Nairz, M., A. Schroll, T. Sonnweber, and G. Weiss. 2010. The struggle for iron - a metal at the host-pathogen interface. *Cell. Microbiol.* 12:1691–1702. http://dx.doi.org/10.1111/j.1462-5822.2010.01529.x

Nairz, M., A. Schroll, A.R. Moschen, T. Sonnweber, M. Theurl, I. Theurl, N. Taub, C. Jamnig, D. Neurauter, L.A. Huber, et al. 2011. Erythropoietin contrastingly affects bacterial infection and experimental colitis by inhibiting nuclear factor-κB-inducible immune pathways. *Immunity.* 34:61–74. http://dx.doi.org/10.1016/j.immuni.2011.01.002

Nemeth, E., and T. Ganz. 2006. Regulation of iron metabolism by hepcidin. *Annu. Rev. Nutr.* 26:323–342. http://dx.doi.org/10.1146/annurev.nutr.26.061505.111303

Nemeth, E., M.S. Tuttle, J. Powelson, M.B. Vaughn, A. Donovan, D.M. Ward, T. Ganz, and J. Kaplan. 2004. Hepcidin regulates cellular iron efflux by binding to ferroportin and inducing its internalization. *Science.* 306:2090–2093. http://dx.doi.org/10.1126/science.1104742

Oexle, H., A. Kaser, J. Möst, R. Bellmann-Weiler, E.R. Werner, G. Werner-Felmayer, and G. Weiss. 2003. Pathways for the regulation of interferon-gamma-inducible genes by iron in human monocytic cells. *J. Leukoc. Biol.* 74:287–294. http://dx.doi.org/10.1189/jlb.0802420

Okada, K., E. Warabi, H. Sugimoto, M. Horie, K. Tokushige, T. Ueda, N. Harada, K. Taguchi, E. Hashimoto, K. Itoh, et al. 2012. Nrf2 inhibits hepatic iron accumulation and counteracts oxidative stress-induced liver injury in nutritional steatohepatitis. *J. Gastroenterol.* 47:924–935. http://dx.doi.org/10.1007/s00535-012-0552-9

Pagani, A., A. Nai, G. Corna, L. Bosurgi, P. Rovere-Querini, C. Camaschella, and L. Silvestri. 2011. Low hepcidin accounts for the proinflammatory status associated with iron deficiency. *Blood.* 118:736–746. http://dx.doi.org/10.1182/blood-2011-02-337212

Paradkar, P.N., I. De Domenico, N. Durchfort, I. Zohn, J. Kaplan, and D.M. Ward. 2008. Iron depletion limits intracellular bacterial growth in macrophages. *Blood.* 112:866–874. http://dx.doi.org/10.1182/blood-2007-12-126854

Richardson, A.R., E.C. Payne, N. Younger, J.E. Karlinsey, V.C. Thomas, L.A. Becker, W.W. Navarre, M.E. Castor, S.J. Libby, and F.C. Fang. 2011. Multiple targets of nitric oxide in the tricarboxylic acid cycle of *Salmonella enterica* serovar typhimurium. *Cell Host Microbe.* 10:33–43. http://dx.doi.org/10.1016/j.chom.2011.06.004

Rothe, H., B. Hartmann, P. Geerlings, and H. Kolb. 1996. Interleukin-12 gene-expression of macrophages is regulated by nitric oxide. *Biochem. Biophys. Res. Commun.* 224:159–163. http://dx.doi.org/10.1006/bbrc.1996.1000

Schaible, U.E., and S.H. Kaufmann. 2004. Iron and microbial infection. Nature reviews 2:946–953. http://dx.doi.org/10.1038/nrmicro1046

Schrettl, M., E. Bignell, C. Kragl, C. Joechl, T. Rogers, H.N. Arst Jr., K. Haynes, and H. Haas. 2004. Siderophore biosynthesis but not reductive iron assimilation is essential for Aspergillus fumigatus virulence. *J. Exp. Med.* 200:1213–1219. http://dx.doi.org/10.1084/jem.20041242

Shiloh, M.U., J.D. MacMicking, S. Nicholson, J.E. Brause, S. Potter, M. Marino, F. Fang, M. Dinauer, and C. Nathan. 1999. Phenotype of mice and macrophages deficient in both phagocyte oxidase and inducible nitric oxide synthase. *Immunity.* 10:29–38. http://dx.doi.org/10.1016/S1074-7613(00)80004-7

Song, M.Y., E.K. Kim, W.S. Moon, J.W. Park, H.J. Kim, H.S. So, R. Park, K.B. Kwon, and B.H. Park. 2009. Sulforaphane protects against cytokine- and streptozotocin-induced beta-cell damage by suppressing the NF-kappaB pathway. *Toxicol. Appl. Pharmacol.* 235:57–67. http://dx.doi.org/10.1016/j.taap.2008.11.007

Sonnweber, T., C. Ress, M. Nairz, I. Theurl, A. Schroll, A.T. Murphy, V. Wroblewski, D.R. Witcher, P. Moser, C.F. Ebenbichler, et al. 2012. High-fat diet causes iron deficiency via hepcidin-independent reduction of duodenal iron absorption. *J. Nutr. Biochem.* 23:1600–1608. http://dx.doi.org/10.1016/j.jnutbio.2011.10.013

Stamler, J.S., and A. Hausladen. 1998. Oxidative modifications in nitrosative stress. *Nat. Struct. Biol.* 5:247–249. http://dx.doi.org/10.1038/nsb0498-247

Tanaka, Y., L.M. Aleksunes, M.J. Goedken, C. Chen, S.A. Reisman, J.E. Manautou, and C.D. Klaassen. 2008. Coordinated induction of Nrf2 target genes protects against iron nitrilotriacetate (FeNTA)-induced nephrotoxicity. *Toxicol. Appl. Pharmacol.* 231:364–373. http://dx.doi.org/10.1016/j.taap.2008.05.022

Theurl, I., V. Mattle, M. Seifert, M. Mariani, C. Marth, and G. Weiss. 2006. Dysregulated monocyte iron homeostasis and erythropoietin formation in patients with anemia of chronic disease. *Blood.* 107:4142–4148. http://dx.doi.org/10.1182/blood-2005-08-3364

Theurl, I., M. Theurl, M. Seifert, S. Mair, M. Nairz, H. Rumpold, H. Zoller, R. Bellmann-Weiler, H. Niederegger, H. Talasz, and G. Weiss. 2008a. Autocrine formation of hepcidin induces iron retention in human monocytes. *Blood.* 111:2392–2399. http://dx.doi.org/10.1182/blood-2007-05-090019

Theurl, M., I. Theurl, K. Hochegger, P. Obrist, N. Subramaniam, N. van Rooijen, K. Schuemann, and G. Weiss. 2008b. Kupffer cells modulate iron homeostasis in mice via regulation of hepcidin expression. *J. Mol. Med.* 86:825–835. http://dx.doi.org/10.1007/s00109-008-0346-y

Vazquez-Torres, A., J. Jones-Carson, P. Mastroeni, H. Ischiropoulos, and F.C. Fang. 2000. Antimicrobial actions of the NADPH phagocyte oxidase and inducible nitric oxide synthase in experimental salmonellosis. I. Effects on microbial killing by activated peritoneal macrophages in vitro. *J. Exp. Med.* 192:227–236. http://dx.doi.org/10.1084/jem.192.2.227

Wang, J., G. Chen, and K. Pantopoulos. 2005. Nitric oxide inhibits the degradation of IRP2. *Mol. Cell. Biol.* 25:1347–1353. http://dx.doi.org/10.1128/MCB.25.4.1347-1353.2005

Wardrop, S.L., R.N. Watts, and D.R. Richardson. 2000. Nitrogen monoxide activates iron regulatory protein 1 RNA-binding activity by two possible mechanisms: effect on the [4Fe-4S] cluster and iron mobilization from cells. *Biochemistry.* 39:2748–2758. http://dx.doi.org/10.1021/bi991099t

Weinberg, E.D. 2000. Modulation of intramacrophage iron metabolism during microbial cell invasion. *Microbes Infect.* 2:85–89. http://dx.doi.org/10.1016/S1286-4579(00)00281-1

Weiss, G. 2009. Iron metabolism in the anemia of chronic disease. *Biochim. Biophys. Acta.* 1790:682–693. http://dx.doi.org/10.1016/j.bbagen.2008.08.006

Weiss, G., and L.T. Goodnough. 2005. Anemia of chronic disease. *N. Engl. J. Med.* 352:1011–1023. http://dx.doi.org/10.1056/NEJMra041809

Weiss, G., D. Fuchs, A. Hausen, G. Reibnegger, E.R. Werner, G. Werner-Felmayer, and H. Wachter. 1992. Iron modulates interferon-gamma effects in the human myelomonocytic cell line THP-1. *Exp. Hematol.* 20:605–610.

Weiss, G., B. Goossen, W. Doppler, D. Fuchs, K. Pantopoulos, G. Werner-Felmayer, H. Wachter, and M.W. Hentze. 1993. Translational regulation via iron-responsive elements by the nitric oxide/NO-synthase pathway. *EMBO J.* 12:3651–3657.

Weiss, G., G. Werner-Felmayer, E.R. Werner, K. Grünewald, H. Wachter, and M.W. Hentze. 1994. Iron regulates nitric oxide synthase activity by controlling nuclear transcription. *J. Exp. Med.* 180:969–976. http://dx.doi.org/10.1084/jem.180.3.969

Yang, F., X.B. Liu, M. Quinones, P.C. Melby, A. Ghio, and D.J. Haile. 2002. Regulation of reticuloendothelial iron transporter MTP1 (Slc11a3) by inflammation. *J. Biol. Chem.* 277:39786–39791. http://dx.doi.org/10.1074/jbc.M201485200

Zhang, D.L., R.M. Hughes, H. Ollivierre-Wilson, M.C. Ghosh, and T.A. Rouault. 2009. A ferroportin transcript that lacks an iron-responsive element enables duodenal and erythroid precursor cells to evade translational repression. *Cell Metab.* 9:461–473. http://dx.doi.org/10.1016/j.cmet.2009.03.006

Zhang, Z., F. Zhang, P. An, X. Guo, Y. Shen, Y. Tao, Q. Wu, Y. Zhang, Y. Yu, B. Ning, et al. 2011. Ferroportin1 deficiency in mouse macrophages impairs iron homeostasis and inflammatory responses. *Blood.* 118:1912–1922. http://dx.doi.org/10.1182/blood-2011-01-330324